

# NEUROCOMPUTATIONAL ANALYSIS AND DESIGN OF DUAL PATCH MICROSTRIP ANTENNA

## A DISSERTATION

*Submitted in partial fulfillment of the  
requirements for the award of the degree*

*of*

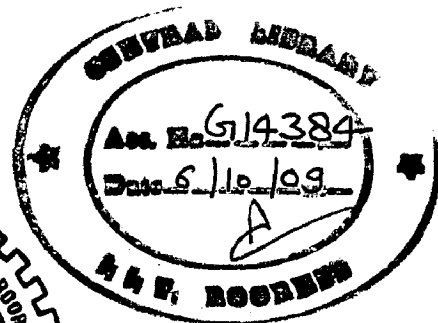
MASTER OF TECHNOLOGY

*in*

ELECTRONICS AND COMPUTER ENGINEERING  
(With Specialization in RF and Microwave Engineering)

*By*

**SUNIL KUMAR YADAV**



DEPARTMENT OF ELECTRONICS AND COMPUTER ENGINEERING  
INDIAN INSTITUTE OF TECHNOLOGY ROORKEE  
ROORKEE-247 667 (INDIA)

JUNE, 2009

## CANDIDATE'S DECLARATION

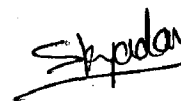
---

I hereby declare that the work that is being presented in this dissertation entitled "NEUROCOMPUTATIONAL ANALYSIS AND DESIGN OF DUAL PATCH MICROSTRIP ANTENNA" in partial fulfillment of the requirements for the award of the degree of **Master of Technology in Electronics & Computer Engineering** with specialization in "RF & Microwave" submitted to the **Department of Electronics & Computer Engineering, Indian Institute of Technology, Roorkee**, is an authentic record of my own work carried under the guidance of **Dr. A. Patnaik, Assistant Professor**, Department of Electronics & Computer, Indian Institute of Technology Roorkee.

The matter embodied in this dissertation has not been submitted for the award of any other degree or diploma.

Date: 30.06.09

Place: Roorkee



SUNIL KUMAR YADAV

---

This is to certify that the above statement made by the candidate is true to the best of my knowledge.



Dr. A. Patnaik

Assistant Professor

E&C Department,

IIT Roorkee, INDIA

## ACKNOWLEDGEMENT

---

It is my proud privilege to express my deep sense of gratitude and sincere thanks towards **Dr. A. Patnaik**, Assistant Professor, Department of Electronics & Computer Engineering, Indian Institute of Technology, Roorkee, for his esteem guidance, and valuable suggestions without which it would not have been possible to compile this dissertation work in present form. This work is simply the reflection of his thoughts, ideas, and concepts. I am highly indebted to him for his kind and valuable suggestions and of course his valuable time during the period of this work. The huge quantum of knowledge I had gained during his inspiring guidance would be immensely beneficial for my future endeavors.

I thank all the teaching and non teaching staff members of the department who have contributed directly or indirectly in successful completion of my dissertation work.

I am extremely grateful to friends and well-wishers for their candid help, meaningful suggestions and persistent encouragement given to me at different stages of my work.

Finally, I would like to say that I am indebted to my parents for everything that they have given to me. I thank them for the sacrifices they made so that I could grow up in a learning environment. They have always stood by me in everything I have done, providing constant support, encouragement and love.

(SUNIL KUMAR YADAV)

Enrollment No:074507

## ABSTRACT

---

Neural network based analysis and design methods of stacked patch antenna have been developed in this dissertation. One of the methods of overcoming the biggest drawbacks of classical microstrip antennas viz narrow bandwidth is to use a stacked microstrip antenna. With the increase in number of layers and radiating patches, the complexity of the analytical/numerical techniques used to analyze these structures also increases. In order to avoid the same, neural network based black-box modeling approach is developed in the present work.

Besides fast response time, the other benefit of using neural networks is that it produces results that are accurate at par with the data used for its training. Two different neural networks have been developed one for analysis and other for the design of dual patch stacked microstrip antennas in the X/Ku band. The job the analysis network is to locate the operational frequencies of the antenna for specific design parameters and the job of the design network is to find the sizes of the radiating patches for the antenna to resonant at the specific frequencies. The training data for the network are generated using IE3D simulation based on method of moment's techniques. The validity of the networks was tested with test data, different from training data and with experiments as well. The developed neural models can be used as CAD packages for analysis and design of stacked patch microstrip antenna.

# CONTENTS

---

<b>CANDIDATE'S DECLARATION</b>	<b>i</b>
<b>ACKNOWLEDGEMENTS</b>	<b>ii</b>
<b>ABSTRACT</b>	<b>iii</b>
<b>CONTENTS</b>	<b>iv</b>
<b>LIST OF TABLES</b>	<b>vii</b>
<b>CHAPTER 1: Introduction</b>	<b>1</b>
1.1 Overview	1
1.2 Motivation	2
1.3 Literature Survey	3
1.4 Organization of Report	4
<b>CHAPTER2: Stacked Microstrip Antenna</b>	<b>6</b>
2.1 Introduction	6
2.2 Characteristics Of MSAs	7
2.2.1 Advantages	7
2.2.2 Disadvantages	7
2.2.3 Application of MSAs	7
2.3 Methods to Analyze Patch Antenna	8
2.3.1 Analytical methods	8
2.3.1.1 Transmission Line Model	8
2.3.1.2 Cavity Model	8
2.3.1.3 Multiport Network Model	9
2.3.2 Numerical methods	9
2.3.2.1 Method of Moments	9
2.4.2.2 Finite Element method	9
2.3.2.3 Finite Difference Time Domain	9
2.4 Different Feeding techniques For MSAs	10
2.4.1 Coaxial Probe Feed	10

2.4.2	Microstrip Line Feed	11
2.4.3	Aperture Coupled Feed	11
2.4.4	Proximity Coupled feed	11
2.5	Multilayer Microstrip Antennas	12
2.5.1	Bandwidth of the Stacked MSAs	13
2.5.2	Two Layer Coaxial Feed ECMSAs	14
2.5.3	Microstrip line Feed ECMSAs	15
2.5.4	Aperture Coupled MSAs	16
2.5.5	Stacked ACMSAs	16
 <b>CHAPTER 3: ANN Basics and Training Algorithm</b>		<b>18</b>
3.1	Introduction	18
3.2	The Neuron Model	18
3.3	Types of Activation Function	20
3.4	Multilayer Perceptrons	21
3.5	Learning in Artificial Neural Networks	22
3.5.1	The Backpropagation Learning Algorithm	22
3.5.2	Flow Chart of Backpropagation Algorithm	24
3.5.3	Summary of the Error Backpropagation Algorithm	25
3.6	Neural Networks in Electromagnetic	26
3.7	Applications in Antennas	26
 <b>CHAPTER 4: Analysis of Stacked Microstrip Antenna</b>		<b>27</b>
4.1	Introduction	27
4.2	Dual Patch Antenna Geometry	27
4.3	ANN Implementation	29
4.3.1	Data Generation	30
4.3.2	ANN Model	30
4.4	Results and Discussion	33

<b>CHAPTER 5: Design of Stacked Microstrip Antenna</b>	<b>40</b>
5.1 Introduction	40
5.2 ANN Implementations	40
5.2.1 Data Generation	40
5.2.2 ANN Model	40
5.3 Results and Discussion	44
<b>CHAPTER 6: Conclusions and Scope for Future Works</b>	<b>48</b>
6.1 Conclusions	48
6.2 Scope for Future Work	48
<b>REFERENCES</b>	<b>49</b>
<b>Appendix I Antenna Fabrication (Wet-Etching Techniques)</b>	<b>53</b>
<b>Appendix II MATLAB Program</b>	<b>57</b>
<b>Appendix III Various Input Parameters of the Dual Patch Microstrip Antenna</b>	<b>60</b>

## LIST OF TABLES

<b>Fig No.</b>	<b>Table Description</b>	<b>Page</b>
4.1	<i>Parameters of the developed neural network model for analysis</i>	32
4.2	<i>Resonant Frequency of Neural Network Model for few Training Data set</i>	33
4.3	<i>Resonant Frequency of Neural Network Model for Test Data Set</i>	34
5.1	<i>Parameters of the developed neural network model for design</i>	42
5.2	<i>Patch Dimensions of neural network model for few training data set</i>	43
5.3	<i>Patch Dimensions of neural network model for test data set</i>	44
App.III	<i>Various Input Parameters of the Dual Patch Microstrip Antenna</i>	60



## Introduction

---

### 1.1 Overview

The concept of microstrip antennas was first proposed by Deschamps 1953 [1]. However, it took nearly two decades to practically implement these antennas, when Munson [2] and Howell [3] developed it in the 1970s. Microstrip patch antennas are resonant antennas with many favorable characteristics, such as low cost, light weight, and low profile. Their main limitation is narrow impedance bandwidth and lower gain. Thus, the impedance bandwidth of a basic patch antenna can be optimized by selecting a low-permittivity substrate, which maximizes the resonant length of the patch, and by maximizing the patch width and substrate thickness. Besides increasing the size, the bandwidth of a microstrip patch antenna can be increased by artificially decreasing its efficiency. However, if the frequency bandwidth could be widened, a broadband microstrip antenna would prove very useful in commercial applications such as mobile satellite communications, 2.5G and 3G wireless system, direct broad cast system (DSB), global system positioning (GPS), wireless local area networks (WLAN), remote sensing and Bluetooth personnel networks.

Microstrip antennas (MSAs), conformal structure, and ease in fabrication and integration with microwave integrated circuit (MIC) or monolithic microwave integrated circuit MMIC) components, have become very popular, not only with researchers but also in industrial applications. Commercial and freeware computer-aided design (CAD) models are available for printed antennas based on various analysis methods. Cavity [4] based models, for patches of regular shapes are electrically thin substrates, use closed-form formulas, and hence are simple and less accurate. Commercial software's [20] use computer intensive numerical methods like FEM, full-wave MoM, and FDTD. It should be robust both for accuracy and computation time point of view.

Much intensive research has been done in the last decade to develop novel bandwidth-enhancement techniques in addition to common techniques of increasing patch height and

decreasing substrate permittivity. These techniques include the utilization of stacked microstrip consisting of several parasitic radiating elements with slightly different size above the driven element (a stacked microstrip patch antenna) [4, 5, 11, 12], a planar patch antenna surrounded by closely spaced parasitic patches (a coplanar parasitic sub array), and incorporation of a dissipative load to lower the Q of the patch. The stacked patch antenna increases the thickness of the antenna height while the coplanar geometry increases the lateral size of the antenna. The bandwidth of single patch antenna can also be increases by implementing internal structures such as shorting pins or slots.

The artificial neural networks (ANN) are data-processing models inspired from the structure and behavior of the biological neurons. They are composed of inter-connected units which we call artificial neurons. The synaptic weights (characteristic elements of the neurons) are modified in the network so that to minimize the obtained error. ANNs are electronic system of hardware or software nature which is built according to the example of a human brain. ANN appeared at the beginning of nineties and they have used for modeling active and passive components, design and optimization of microwave circuit, modeling of microstrip antennas, reverses modeling of microwave devices, and automatic impedance matching etc. Using ANN microwave engineers have simplified a rather difficult and time consuming design of microwave system. This report aim at describing the role of ANNs in printed antenna modeling.

The neural networks have been introduced for antenna modeling, simulation, and optimization. Fast, accurate, and reliable neural network models can be developed from measured/simulated microwave data. The third chapter of this report describes the basics of neural network technique. The Back propagation training algorithm, which is the most widely used training algorithm is antenna modeling in described in detail in chapters-3[21-23].

## **1.2 Motivation**

The explosive growth in broadband/multiband wireless communications systems has increased the demands to enhance information accessibility and created a need for more bandwidth-efficient communication techniques. One of the ways to get the multiband/wide band effect in microstrip antennas is to use a stacked microstrip antenna configuration. Stacked configurations have also been proved as a suitable candidate for reflect array applications.

The number of design parameters increases with the increase in layers of the stacked configuration, thereby increasing the simulation time in the available commercial simulators. In order to optimize these structures, it needs several simulations before landing up in a final solution. Therefore in order to reduce the optimization time, we thought of developing a fast CAD model for analysis and design of stacked microstrip antennas. Because neural networks are capable of handling large number of input/output parameters in forming black-box modeling and at the same time, their response is fast, so in this present work, we have used the same technique to develop to models viz. (i) to find out the resonant frequencies of stacked microstrip antennas and (ii) to find out the dimensions of the patches for the antenna to resonate at specific frequencies.

### 1.3 Literature Survey

**Papiernik [9]:** Multilayer microstrip antennas fed by coaxial probe or microstrip line has been studied in this paper. It discusses different structures with stacked or offset radiating elements of various shapes including rectangles, discs and triangles. Theoretical and experimental results of input impedance are given for the different structures. Radiation information is presented and the relative merits of different structures are discussed.

**Sabban [10, 14]:** In these papers, a new stacked two-layer antenna is introduced. It has a bandwidth of 25 to 35% for VSWR of 2: 1 or better which is achieved with thick and lower dielectric constant. It is fed directly by transmission line by bottom patch; the radiating element is excited electromagnetic coupling by a feeding element.

**Davidovitz [13]:** It gives guidelines for design of electromagnetically coupled square and circular microstrip antennas. The substrates of two different dielectric layers are considered, the analysis is extended to electrically thick substrates. The design data were computed by applying the MoM in the spectral domain to solve the integral equation for the currents on the patch and portion of the microstrip feed line. The integral equation was formulated using the appropriate dyadic Green function for the grounded multilayered slab.

**Waterhouse [17]:** It presents a variation of the aperture-coupled stacked patch microstrip antenna, which greatly enhances its bandwidth. The impedance bandwidth of this antenna is compared

with that of other wide-band microstrip radiators. The effects of varying the size, shape and dimension of the patch and its slot of the antenna are investigated.

**Pozar [18]:** This paper presents the experimental results for a proximity coupled microstrip patch antenna capable of giving 13% bandwidth. The impedance match ( $VSWR < 2$ ), co-polarized radiation patterns and cross-polarized radiation were measured over this bandwidth. Microstrip feed line on a substrate are used to proximity-coupled to a rectangular microstrip patch antenna.

**Crop & Papiernik [19]:** This paper presents two types of feeds, the coaxial probe and slot coupling, used to obtain broadband operation in multilayer microstrip antennas are compared,. It is used to develop a model for the antennas and the radio characteristics obtained in the frequency bands (X/Ku) of the applications for these antennas.

**Somasiri *et. al.* [24]:** It proposes a numerical modeling of a dual band multilayered microstrip patch antenna operating at 35 GHz. The simulated and measured resonant frequencies of both lower and upper patch are compared to check the accuracy of the different numerical modeling techniques.

**Somasiri *et. al.* [26]:** It presents the development of a neural network modeler for the optimization of a dual band multilayer microstrip patch antenna. The developed neural modeler speeds up design optimization by replacing repeated EM simulations and retains good accuracy compared with the MOM modeling.

**Guney & sagiroglu [30]** have been presented a generalized method for accurate determination of the resonant frequencies of microstrip antennas, based on the multilayered perceptrons network. Three learning algorithms, backpropagation, delta-bar-delta, and extended delta bar delta are used to train perceptrons. Neural results for the resonant frequencies of the rectangular, circular and triangular microstrip antennas are in good agreement with the experimental results.

**Krishna *et. Al.* [38]** has presented a simple and accurate ANN models for the synthesis and analysis of Microstrip lines, which provide circuits that are compact and light in weight, to more accurately compute the characteristic parameters and the physical dimensions respectively for the required design specifications.

## **1.4 Organization of Report**

There are six chapters compiled in this dissertation including the present chapter.

The next chapter discusses the basics of the microstrip antennas including the stacked version microstrip antenna. In chapter 3, a brief discussion of the basic concept of ANN and the backpropagation training algorithm is presented. Chapter 4 and 5 describes the analysis and design of stacked microstrip antennas using the neural networks technique, respectively. In these chapters the training data generation process, ANN implementation and the results obtained are discussed. Finally concluding remarks along with future research directions were outlined.

## Stacked Microstrip Antenna

This chapter describes the basics and the demerits of a single layer microstrip antenna. The different analysis method for microstrip antenna is briefly outlined. The requirement of stacked patch antennas and their different forms are described.

### 2.1 Introduction

In its most basic form, a microstrip patch antenna consists of a radiating patch on one side of a dielectric substrate which has a ground plane on the other side. The patch made of conducting material such as copper or gold and can take any possible shape. The top and side views of a *rectangular Microstrip Antenna (RMSA)* are shown fig: 2.1.

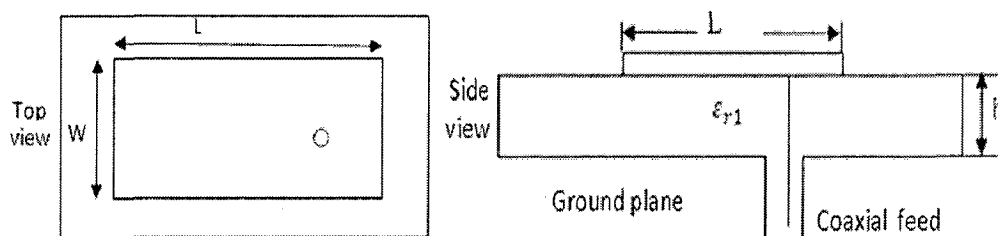


**Fig: 2.1** MSA Configurations (a) top view (b) side view

The patch is generally square, rectangular, circular, triangular, and elliptical or some other common shape as shown in Fig: 2.2.

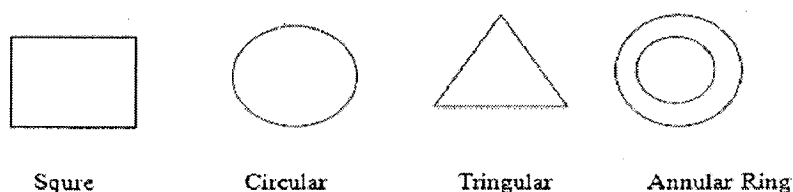


**Fig: 2.2** Different Shapes of Microstrip Patches

Microstrip patch antennas radiate primarily because of the fringing fields between the patch edge and the ground plane. For good antenna performance, a thick dielectric substrate having a low dielectric constant is provides better efficiency, larger bandwidth and better radiation. To enhance the fringing fields from the patch, the width  $W$  of the patch is increased. The fringing fields are also enhanced by decreasing the  $\epsilon_r$ , or by increasing the substrate thickness  $h$ .

## **2.2 Characteristics of MSAs**

The MSA has proved to be an excellent radiator for many applications because of its several advantages, but it also has some disadvantages.

### **2.2.1 Advantages**

- They are light weight and have a small volume and a low-profile planar configuration.
- They can be made conformal to the host surface.
- Their ease of mass production using printed-circuit technology leads to a low fabrication cost.
- They are easier to integrate with other MICs on the same substrate.
- They allow both linear polarization and circular polarization.
- They can be made compact for use in personal mobile communication.
- They allow for dual- and triple-frequency operations

### **2.2.2 Disadvantages**

- Narrow BW
- Low power-handling capability
- Lower gain

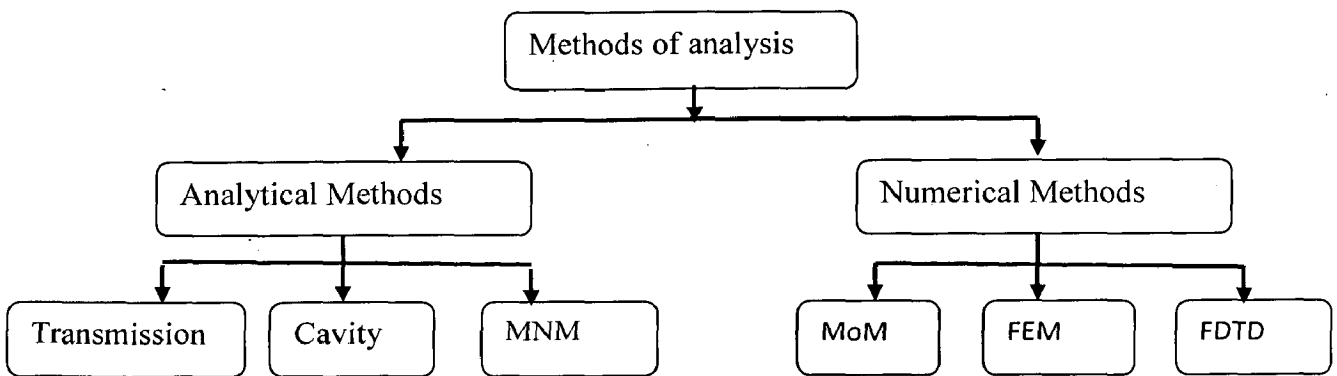
### **2.2.3 Application of MSAs**

The advantages of MSAs make them suitable for numerous applications. The telemetry and communications antennas on missiles need to thin and conformal. Smart weapon system use

patches antennas because they provide thin profile. Pagers, GSM, GPS, are the major users of patch antennas.

### 2.3 Methods to Analyze Patch Antenna

The patch antenna has a two-dimensional radiating patch on a thin dielectric substrate and they are categorized as a two-dimensional planar structure for analysis purposes. The analysis methods for MSAs can be broadly divided in two groups shown in the chart:



#### 2.3.1 Analytical methods

##### 2.3.1.1 Transmission Line Model

The transmission line model views the patch or microstrip radiator as a transmission line resonator with no transverse fields and radiation mainly occurs from the fringing fields at the open circuited ends. The patch is represented by two slots that are spaced by the length of the resonator.

Although the transmission line model is easy to use, all types of configurations cannot be analyzed using this model since it does not take care of variation of field in the orthogonal direction to the direction of propagation.

##### 2.3.1.2 Cavity Model

In the cavity model, the region between the patch and the ground plane is treated as a cavity that is surrounded by magnetic walls around the periphery and by electric walls from the top and



bottom sides. Since thin substrates are used the field inside the cavity is uniform along the thickness of the substrate. The far-fields and the radiation are computed by the equivalent magnetic current around the periphery.

### **2.3.1.3 Multiport Network Model**

In this method, the electromagnetic fields underneath the patch and outside the patch are modeled separately. The patch is analyzed as a two-dimensional planar network, with a multiple number of ports located around the periphery. The multiport impedance matrix of the patch is obtained from its two-dimensional Green's function. The segmentation method is then used to find the overall impedance matrix. The radiated fields are obtained from the voltage distribution around the periphery is used to obtain far fields and radiation.

## **2.3.2 Numerical methods**

### **2.3.2.1 Method of Moments**

The method of moments is one of the most commonly used numerical techniques. In the MoM, the surface currents are used to model the microstrip patch. An integral equation is formed that is expanded in terms of some basis and testing functions are transformed into a matrix form that can be easily solved by a computer. This method takes into account effect of fringing fields hence provide more exact solution.

### **2.3.2.2 Finite Element method**

Finite element method is suitable for volumetric configuration. In this method, the region of interest is divided into any number of finite surfaces. These discretized units, may be any well-defined geometrical shapes such as triangular, tetrahedral elements for planar configurations, 2D or 3D. This method is very handy when the shape of the patch is arbitrarily. But its only limitation is that it needs a truncation boundary to be applied.

### **2.3.2.3 Finite Difference Time Domain**

Finite Difference Time Domain method conveniently models patch antennas. It utilizes spatial as well as time grid for electric and magnetic fields over which solution is required. The entire domain is divided into small units called cells. The Maxwell's equations in differential form are used in this method. The discrete time variations of the fields are determined at desired locations. Using line integral of electric fields the voltage across two locations can be obtained. The current is computed by using loop integral of magnetic field.

## 2.4 Different Feeding techniques For MSAs

Feeding techniques for patch can be classified as:

1. Direct feeding techniques
  - a) Coaxial probe excitation
  - b) Microstrip line feed
2. Indirect feeding techniques
  - a) Aperture coupled feed
  - b) Proximity coupled feed
  - c) Coplanar waveguide feed

### 2.4.1 Coaxial Probe Feed

The coaxial probe feed is most commonly used feeding technique. The figure 2.3 has shown the coaxial feed. The center conductor is soldered to the patch and outer conductor to the ground plane. The main advantage of this feed is that it can be placed at any desired location inside the patch to match the input impedance.

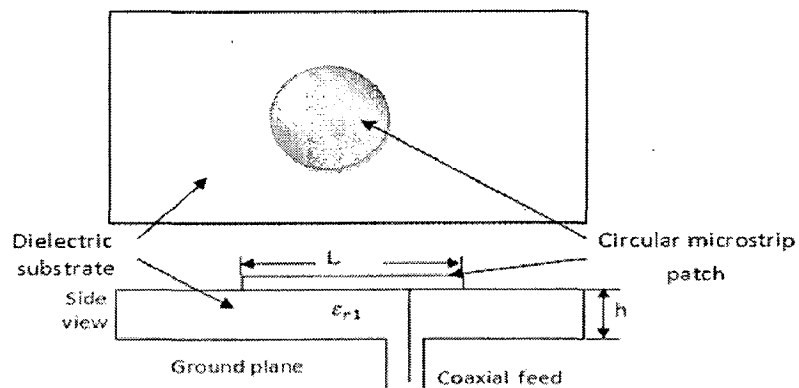


**Fig: 2.3**Probe fed Circular Microstrip Patch Antenna

### 2.4.2 Microstrip Line Feed

A patch with microstrip line feed is shown in figure 2.4. This feed arrangement has an advantage that it can be etched on the substrate so the structure remains planar. Also the drawback is radiation from feed line which leads to increase in cross polar level.

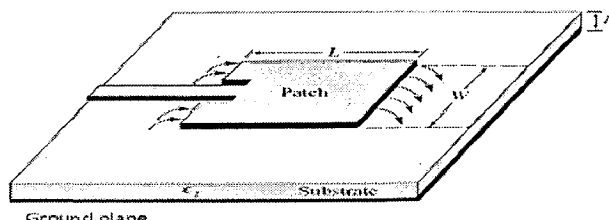


Fig: 2.3 Microstrip Line Feed

### 2.4.3 Aperture Coupled Feed

This is an indirect feeding technique in which the field is coupled from the microstrip line feed to the radiating patch through a small aperture or slot cut in the ground plane, as shown in figure 2.5. The coupling aperture is usually centered under the patch, leading to the lower cross polarization due to symmetry of the configuration.

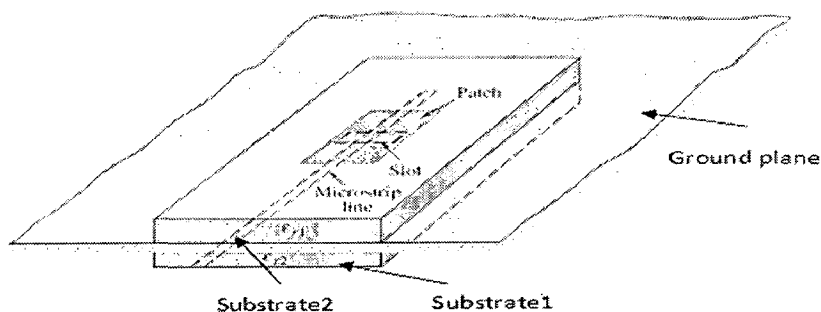
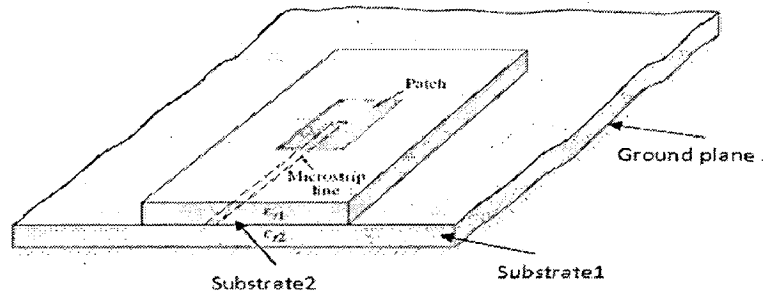


Fig: 2.5 Aperture-coupled feed

### 2.4.4 Proximity Coupled feed

This technique utilizes the electromagnetic coupling principle. The microstrip line feed is placed between the patch and the ground plane separated by two dielectric layers. The advantage of this feed is that it eliminates the spurious radiations due to feed network as the feeding layer and radiation layer are isolated



**Fig: 2.6 Proximity-coupled Feed**

## 2.5 Multilayer Microstrip Antennas

The Microstrip patch antennas has proved to be an excellent radiator for many applications because of its several advantage, but it also has some disadvantage like narrow bandwidth, lower gain, low power handling capability etc. MPAs have inherently narrow bandwidth, typically 1-5%, which is the major limiting factor for the application of these antennas. Increasing the bandwidth of MPAs has a major area of research.

The bandwidth of the MSAs can be increased by

1. Increasing substrate thickness
2. Decreasing the dielectric constant
3. Coupling resonators in planar or stacked configurations

Phenomenon of stacking is based on the concept of resonant circuits where coupling occurs between patch element and parasitic elements which are tuned to slightly different frequencies. There are two limitations are planar coupled resonators. 1) the overall size of the antenna increases and 2) the radiation pattern may vary over the range of frequency. Hence using stacked configuration techniques, two or more patches on different layers of the dielectric substrates are stacked on each other. This method increase the overall height of the antenna but the size in the planar direction remains the same as that of the single patch antenna. This technique can yield up to 70% ( $VSWR \leq 2$ ) bandwidth and the variation of the radiation pattern over the impedance bandwidth is small.

Some of the important characteristics of the stacked microstrip antennas are follows.

### 2.5.1 Bandwidth of the Stacked MSAs

The bandwidth can be defined in terms of its VSWR or input impedance variation with frequency or in terms of radiation pattern parameters. For the circularly polarized antenna, bandwidth is also defined in terms of axial ratio (AR).

The impedance bandwidth is commonly defined as the 'frequency range over which VSWR is less than a pre-specified value usually 2:1 (return loss 9.5 dB or 11% reflected power)'. The bandwidth of the MSAs is inversely proportional to its quality factor Q and is given by [7].

$$BW = \frac{VSWR - 1}{Q\sqrt{VSWR}} \quad (2.1)$$

The expressions for approximately calculated the percentage bandwidth of the rectangular microstrip antenna in terms of patch dimensions ( $L$ ,  $W$ ) and substrate parameters ( $\epsilon_r$ ) is given by [3]

$$\%BW = \frac{Ah}{\lambda_0} \sqrt{\frac{W}{L}} \quad (2.2)$$

Where

$$A = 180 \text{ for } \frac{h}{\lambda_0\sqrt{\epsilon_r}} \leq 0.045$$
$$A = 220 \text{ for } 0.045 \leq \frac{h}{\lambda_0\sqrt{\epsilon_r}} \leq 0.075$$
$$A = 220 \text{ for } \frac{h}{\lambda_0\sqrt{\epsilon_r}} \geq 0.075$$

Bandwidth enhancement can be achieved by using electrically thick substrate and reducing substrate permittivity. Increasing substrate thickness reduces the Q of the antenna so improve bandwidth. But it reduces compactness, increases cross polarization and increase surface wave excitation, which deteriorates the quality of the radiation. Electrically thick

microstrip patch antenna elements are difficult to excite at microwave frequency. A feeding technique has been discussed earlier, if the element is fed by a coaxial probe, probe introduces a series inductive reactance proportional to the substrate thickness, which prevents proper matching.

In case of stacked microstrip antenna it has increases the overall height of the antenna but size in the planar direction remains the same as that of the single patch antenna. Based on the coupling mechanism, these configurations are categorized as electromagnetically coupled MSAs (ECMSAs) and aperture-coupled MSAs (ACMSAs). These multilayer MSA configurations yield BW of nearly 70% for  $VSWR \leq 2$ , and the variation of the radiation pattern over the impedance BW is small [4, 5,6,11,12].

### 2.5.2 Two Layer Coaxial Feed ECMSAs

The two configurations of an ECMSA are shown in figure 2.7. The bottom patch is fed by with a coaxial line, and the top parasitic patch is excited due to electromagnetic coupling with the bottom patch. The patches can be fabricated on different substrates, and an air gap or foam material can be introduced between these layers to increase the BW. In the normal configuration, as shown in Figure 2.7(a), the parasitic patch is on the upper side of the substrate. In the inverted configuration shown in Figure 2.7(b), the top patch is on the bottom side of the upper substrate. In this case, the top dielectric layer also acts as a protective layer from the environment. The antenna dimensions are optimized so that the resonance frequencies of the two patches are close to each other to yield broad BW.

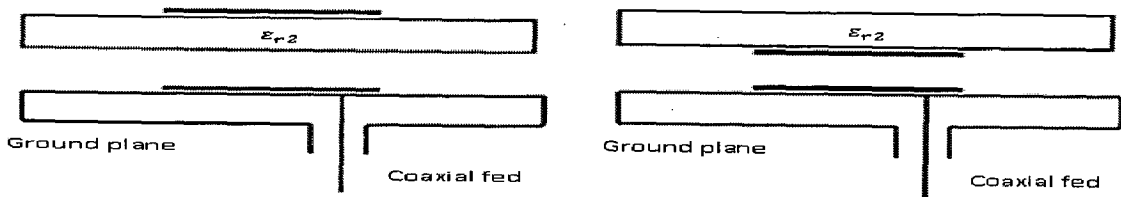


**Fig 2.7:** Electromagnetically coupled MSA: (a) normal and (b) inverted configurations

The top patch can be fed by coaxial probe, which passes through the bottom patch as shown in Fig: 2.8. The bottom patch is not directly connected with the probe. It gets excited through the electromagnetic coupling arising from the probe and the upper patch. This

configuration does not offer any advantage as compared to the configurations given in figure 2.7.



Fig: 2.8 ECMSA with feed connected with top patch

### 2.5.3 Microstrip line Feed ECMSAs

The microstrip line feed in the bottom layer as shown in Fig: 2.9. This configuration has the advantage that the microstrip feed line could be fabricated on a thin high dielectric constant substrate, so that radiation from the feed is negligible and the top patch can be fabricated on a thick substrate with a low dielectric constant (or suspended configuration) for a large BW. Also, there is no direct connection between the feed and the patch. A small misalignment between the patch and the feed, unlike in the case of coaxial feed where it is very critical, does not change the characteristics of the antenna.

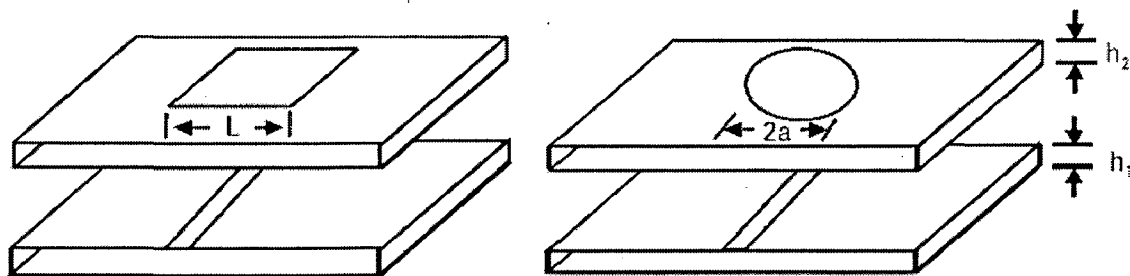
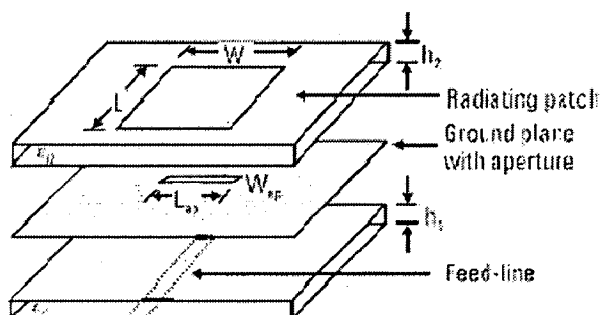


Fig: 2.9 ECMSA with microstrip line feed (a) rectangular (b) circular patch

### 2.5.4 Aperture Coupled MSAs

It was first proposed in 1985 for enhancement of the BW of the MSA [5]. By optimizing the various parameters including the aperture dimensions, a BW of nearly 70% has been achieved. An ACMSA consists of two substrates separated by a ground plane shown in fig: 2.10. The top substrate contains the radiating element, and the bottom

substrate contains the microstrip feed line. A small aperture is cut in the ground plane to allow coupling from the open-circuited microstrip feed line to the radiating patch as shown in fig 2.10.



**Fig: 2.10** Single layer aperture coupled MSA

The ACMSA has several advantages:

- The top patch could be fabricated on a thick low dielectric substrate to enhance the BW, and the feed network on the other side of the ground plane could be on a thin high dielectric substrate to reduce radiation losses.
- Radiation from the feed network does not interfere with the main radiation pattern, since the ground plane separates the two substrates.
- The excess reactance of the antenna can be compensated for by varying the length  $L_s$  of the open-circuited microstrip stub.
- The input impedance is easily controlled by the size, shape, and position of the aperture.

The ACMSA also has certain disadvantages. The total thickness of the antenna is large as compared to a probe-fed MSA. Also, the back radiation occurs more through the coupling aperture in the ground plane, which can be reduced by using a small aperture.

### 2.5.5 Stacked ACMSAs

A larger BW of 50–70% is obtained if the stacked patches are fed with a resonant aperture. The air gap has been used between the patch and the ground plane and between the two patches, which increases the total thickness of the ACMSA and hence its BW. For the case of two stacked patches with a resonant slot, two loops are formed,



representing the interaction between three resonators (two patches and one resonant slot). This configuration is also known as an aperture-stacked patch shown in fig: 2.11.

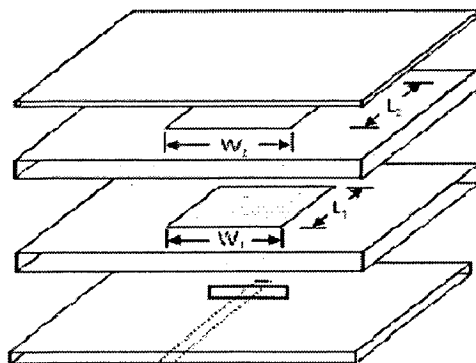


**Fig: 2.11** Multilayered aperture- stacked square patch antenna

## ANN Basics and Training Algorithm

### 3.1 Introduction

Artificial neural networks are one of the tools for artificial intelligence and they have been inspired and motivated from the organization of the real, biological brain. The human brain is considered as a highly complex, nonlinear, and massively parallel information-processing device, perform many tasks like memory, learning, construction of its own experimental rules. The algorithm that provides the learning ability to the network is based on the synaptic weights modification of the neural interconnections, and is called learning algorithm.

A neural network is a massively parallel distributed processor made up simple processing units, which has a natural propensity for storing experimental knowledge. It resembles the brain in two respects (Haykin 1998) [21]:

1. Knowledge is acquired by the network through a learning process.
2. Interconnection strengths known as synaptic weights are used to store the knowledge.

### 3.2 The Neuron Model

A neuron is an information-processing unit of an NN. The simplest model of the neuron shown in Figure 3.1 consists of the three basic elements of the neuronal model: a set of synapses or synaptic links, an adder (logical unit) and activation function (threshold function).

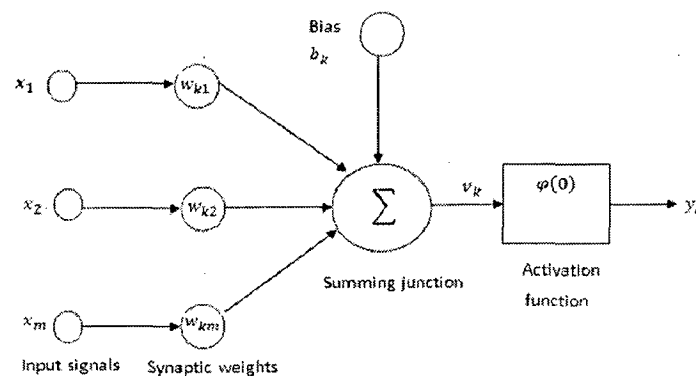


Fig: 3.1 Model of a neuron [21]

1. A set of synapses or connecting links carry the input signals to the neuron, coming from either the environment or outputs of other neurons. Each synapse is characterized by a weight or strength.
2. The second basic element of the model neuron is the adder. This element is responsible for summing the input signals to the neuron that are transmitted through the synapses of the neuron. The total result of the summation of the incoming weighted signal and the addition of the bias  $b_k$  or subtraction of the threshold  $\theta_k$  is denoted by  $v_k$ .
3. The third basic element of the model neuron is the activation function, an activation function for limiting the amplitude of the output of a neuron: which is also referred as squashing function or signal function.

The model of neuron in Fig 3.1 also includes an externally applied threshold  $\theta_k$ , the  $k_{th}$  neuron receives  $m$  synaptic connections,  $v_k$  is the total sum of the incoming input weighed signals  $x_j$  via the  $k_{th}$  synaptic connection, and  $w_{kj}$  is the corresponding synaptic weights, the threshold is  $\theta_k$  and the bias is  $b_k$ . In the case that the adder sums the total incoming weighted signals and subtracts the threshold  $\theta_k$  the obtained result  $v_k$  is given by the mathematical formula:

$$v_k = \sum_{j=1}^m w_{kj} \quad (3.1)$$

In the case that the adder sums the total incoming weighted signals and the weighted bias  $b_k$ , the total result  $v_k$  is given by a formula similar to

$$v_k = \sum_{j=1}^m w_{kj} x_j + b_k \quad (3.2)$$

The last formula can be modified slightly to a more compact form:

$$v_k = \sum_{j=0}^m w_{kj} x_j \quad (3.3)$$

Finally, let  $y_k$  be the output signal of the  $k_{th}$  neuron that receives a total incoming signal  $v_k$ . The output of the neuron is given by the next formula:

$$y_k = \varphi(v_k) \quad (3.4)$$

In the above equation,  $\varphi(v)$  is the activation function, which should be given by one of the described in Eqs. 3.5 – 3.8.

### 3.3 Types of activation Function

The activation function defines the output of the neuron in terms of the induced local field  $v$ . There are three basic types of activation functions.

#### 1. Threshold function:

$$\varphi(v) = \begin{cases} 1 & \text{if } v \geq 0 \\ 0 & \text{if } v < 0 \end{cases} \quad (3.5)$$

This form of the threshold function is commonly referred to as a Heaviside function. The output of the neuron  $k$  employing such a threshold function is expressed as

$$y_k = \begin{cases} 1 & \text{if } v_k \geq 0 \\ 0 & \text{if } v_k < 0 \end{cases} \quad (3.6)$$

Where  $v_k$  the induced local is field of the neuron; is that

#### 3. Piecewise Linear Function:

For the piecewise linear function described, we have the piecewise-linear function reduces to a threshold function if the amplification factor of the linear region is made infinitely large.

$$\varphi(v) = \begin{cases} 1, & v \geq +\frac{1}{2} \\ v, & +\frac{1}{2} > v > -\frac{1}{2} \\ 0, & v \leq -\frac{1}{2} \end{cases} \quad (3.7)$$

#### 3. Sigmoid function:

The sigmoid function, whose graph is s-shaped, is by far the most common form of activation function used in the construction of the artificial neural networks. An example of the sigmoid function of the logistic function, defined by

$$\varphi(v) = \frac{1}{1 + \exp(-av)} \quad (3.8)$$

Where 'a' is the slope parameter of the sigmoid function.

### 3.4 Multilayer Perceptrons

The networks consist of a set of input layer, one or more hidden layers and output layer of computation nodes. The input signal propagates through the network in a forward direction, on a layer-by-layer basis. These neural networks are commonly referred to as MLPs. Multilayer perceptrons have been applied successfully to solve the some difficult and diverse problem by training them in a supervised manner with a highly popular algorithm known as the error back-propagation algorithm.

A multilayer perceptrons has three distinctive characteristics.

- The model of each neuron in the network includes a nonlinear activation function. The commonly used form of nonlinearity that satisfies this requirement is a sigmoid nonlinearity defined by the logistic function.
- The network contains one or more layers of hidden neurons that are not part of the input or output of the network. These hidden neurons enable the network to learn complex task by extracting progressively.
- The network exhibits a high degree of connectivity, determined by the synapses of the network.

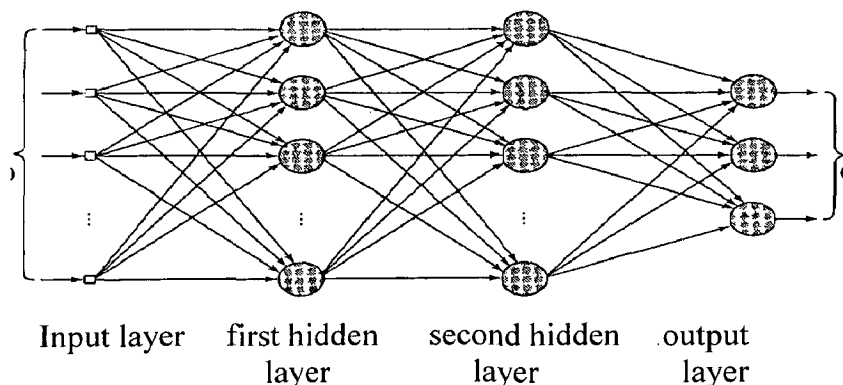


**Fig: 3.2** Multilayer perceptron with two hidden layer

### 3.5 Learning in Artificial Neural Networks

Thus, learning is the process by which a neural network modifies its internal structure in response to external stimuli. The prescribed set of well-defined rules that specifies these structural modifications in the network for the solution of a learning problem is called a learning algorithm, learning law, or learning rule.

The algorithm is based on the back propagation of the errors, the differences between the actual and the desired output and is the most commonly used generalization of the Delta Rule. The algorithm involves two phases, the forward phase that occurs when the inputs are presented to the neurons of the input layer and are propagated forward to compute the output and the backward phase, when the algorithm performs modifications in the backward direction.

#### 3.5.1 The Back-Propagation Learning Algorithm [9-11]

The Back-Propagation Learning Algorithm is applied on multilayer feed forward networks, also referred as multilayer perceptrons (MLP). It is based on an error correction learning rule and it is the minimization of the mean squared error that is a measure of the difference between the actual and the desired output. In a multilayer feed forward networks, the multilayer perceptrons are constructed of at least three layers, one input layer, one or more hidden layers and one output layer, each layer consisting of elementary processing units, which is a nonlinear activation function, commonly the logistic sigmoid function for hidden layers and linear for output layer.

The Back-Propagation Learning Algorithm calculates the difference between the actual response and the desired output of each neuron of the output layer of the network. Assuming that  $y_j(n)$  is the actual output of the  $j_{th}$  neuron of the output layer and  $d_j(n)$  is the corresponding desired output, the error signal  $e_j(n)$  is defined as:

$$e_j(n) = d_j(n) - y_j(n) \quad (3.10)$$

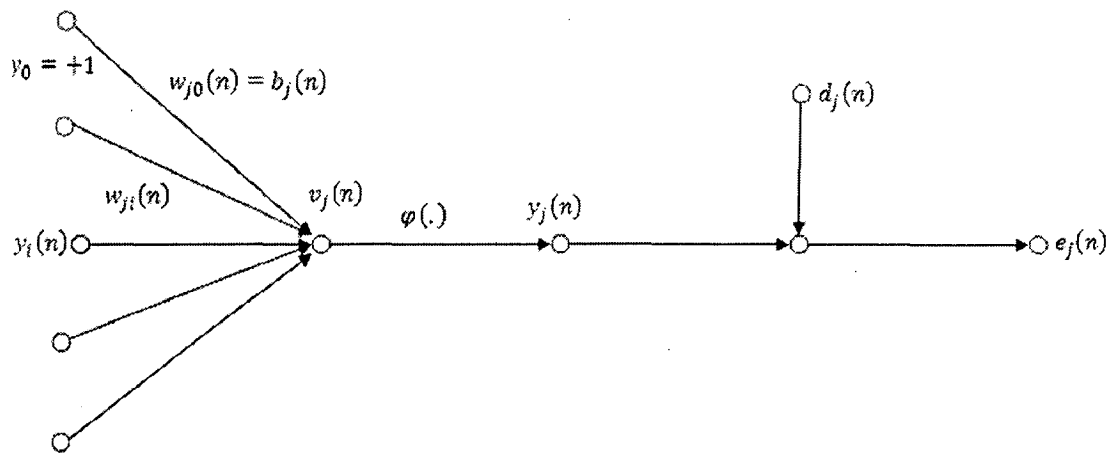


**Fig: 3.3** Signal flow graph error Backpropagation Algorithm

We now summarize the relations that we have derived for the back-propagation algorithm. First, the correction  $\Delta w_{ji}(n)$  applied to the synaptic weight connecting neuron  $i$  to neuron  $j$  is defined by the delta rule:

### 3.5.3 Summary of the error backpropagation training algorithm

Given are P training pairs

$$\{z_1, d_1, z_2, d_2, \dots, z_p, d_p\}$$

Where  $z_i$  is  $(I \times 1)$ ,  $d_i$  is  $(K \times 1)$ , and  $I = 1, 2, \dots, P$ .

**Step 1:**  $\eta > 0$ ,  $E_{max}$  chosen.

Weights  $W$  and  $V$  are initialized at small random values;  $W$  is  $(K \times J)$ ,  $V$  is  $(J \times I)$ .

**Step 2:** Training step start here

Input is presented and the layers outputs computed.

$$y_j \leftarrow f(V_j^t Z), \text{ for } j = 1, 2, \dots, J$$

$$o_k \leftarrow f(W_k^t y), \text{ for } k = 1, 2, \dots, K$$

**Step 3:** Error values is computed.

$$E \leftarrow \frac{1}{2} (d_k - o_k)^2 + E, \text{ for } k = 1, 2, \dots, K$$

**Step 4:** Error signal vector  $\delta_o$  and  $\delta_y$  of both layers are computed.

$$\text{Vector } \delta_o \text{ is } (K \times 1), \delta_y \text{ is } (J \times 1)$$

The error signal terms of the output layer in this step are.

$$\delta_{ok} = \frac{1}{2} [(d_k - o_k)(1 - o_k^2)], \text{ for } k = 1, 2, \dots, K$$

The error signal terms of the hidden layer in this step are

$$\delta_{yj} = \frac{1}{2} (1 - y_j^2) \sum_{k=1}^K \delta_{ok} W_{kj}, \text{ for } j = 1, 2, \dots, J$$

**Step 5:** Outputs layer weights are adjusted:

$$W_{kj} = W_{kj} + \eta \delta_{ok} y_j, \text{ for } k = 1, 2, \dots, K \text{ and } j = 1, 2, \dots, J$$

**Step 6:** Hidden layer weights are adjusted.

$$V_{ji} \leftarrow V_{ji} + \eta \delta_{yj} z_i, \text{ for } j = 1, 2, \dots, J \\ I = 1, 2, \dots, I$$

**Step 7:** If  $p < P$  then  $p \leftarrow p + 1$ ,  $q \leftarrow q + 1$ , and go to step 2, otherwise go to step 8.

**Step 8:** Training cycle is completed.

For  $E < E_{max}$  terminate the training session. Output weights  $W$ ,  $V$ ,  $q$  and  $E$ .

If  $E > E_{max}$ , then  $E \leftarrow 1$ ,  $q \leftarrow 1$ , and initiate the new training cycle by going to step 2.



### 3.5.2 Flow Chart of the back propagation Algorithm

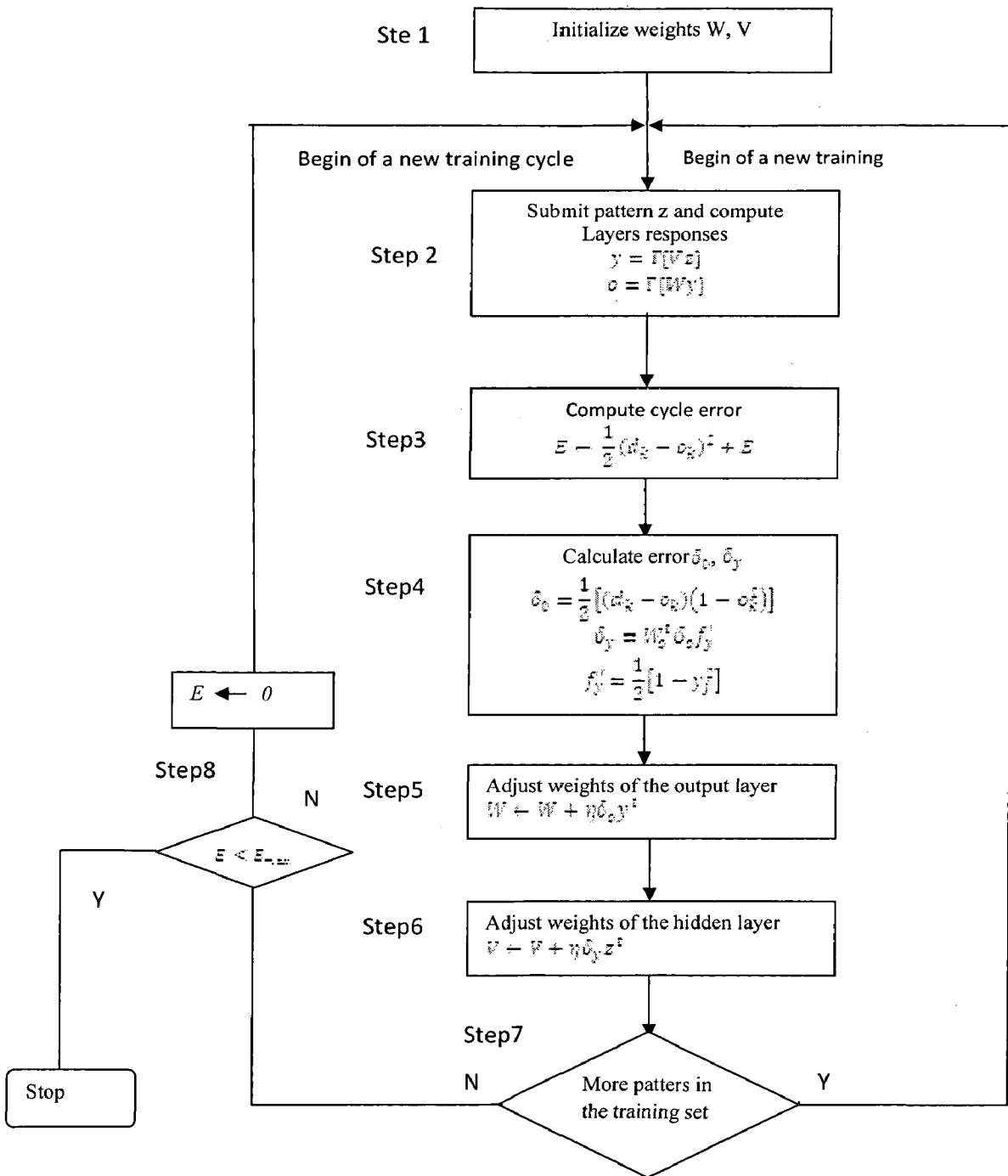


Fig: 3.4 Flow Chart of the back propagation Algorithm

### **3.6 Neural Networks in Electromagnetic**

There are four main situations in which NNs are used in electromagnetic:

1. When closed form solutions do not exist, and trial –and-error methods are the main approaches to tackling the problem at hand.
2. When an application requires real time performance.
3. When faster convergence rates are required in the optimization of large system.
4. When enough measured data exist to train an ANN for prediction purpose, especially when no analytical tools exist.

### **3.7 Applications in Antennas**

Neural networks have been used for antenna applications. The following are some of those applications:

1. Varying the usable bandwidth of microstrip patch antennas. [11]
2. Estimating the angle of arrival of signals in a mobile communications environment. [7]
3. Determining the excitation coefficient in phased array antennas to change the direction of the radiation beam for target tracking. [6]
4. Designing frequency selective surface to be used as dichotic reflectors. [4]
5. Compensating for surface errors in reflector antennas. [5]
6. Predicting radiations from nonuniform reflecting surfaces and the others applications. [4]

## **Analysis of Stacked Microstrip Antenna**

---

### **4.1 Introduction**

In this chapter, a neural network modeler is developed for locating the resonant frequencies of a dual patch stacked microstrip antenna. The developed neural network takes different design parameters of the antenna as input and delivers the lower and upper resonant frequencies. The validity of the network is tested with simulations from IE3D as well as with experimental results. The following section describes the structure of the antenna, training data generation process, neural network training process and finally discusses the results.

### **4.2 Dual Patch Antenna Geometry**

The basic structure used for the analysis is shown in Fig. 4.1. Two square patches were used. The lower patch was coaxially fed and the upper patch is covered by another dielectric layer acting as a protective layer. The values of the design parameter were fixed in such a way, so that the antenna can resonate in X/Ku band. The initial values were chosen according to [19]. The values are  $W_1 = L_1 = 8\text{mm}$ ,  $W_2 = L_2 = 6.9\text{mm}$ ,  $\epsilon_{r1} = 2.2$ ,  $\epsilon_{r2} = 1$ ,  $\epsilon_{r3} = 2.2$ ,  $h_1 = 1.53\text{mm}$ ,  $h_2 = 1.53\text{mm}$ ,  $h_3 = 3.09\text{mm}$ ,  $x_p = y_p = 2.5\text{mm}$ . With these values, the operating frequencies of the antenna were  $f_l = 11.53\text{ GHz}$  and  $f_u = 16.93\text{ GHz}$ .

The reason of choosing this coaxial feeding method is chosen mainly due to its easy fabrication process. Other advantages of coaxial feeding are its robust nature, can be placed at any desired location for input impedance matching, good isolation between the feeding network and the radiating element that contributes to a good front to back ratios and minimum misalignment difficulties due to direct contact between the probe and the patch.

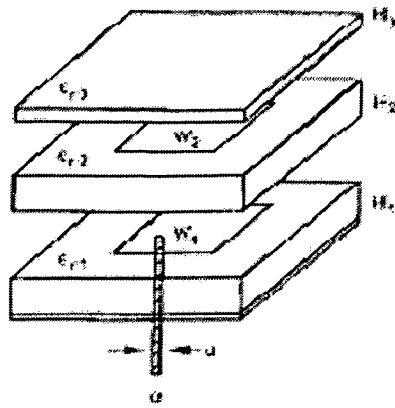


**Fig: 4.1** Coaxial fed dual patch microstrip antenna [19]

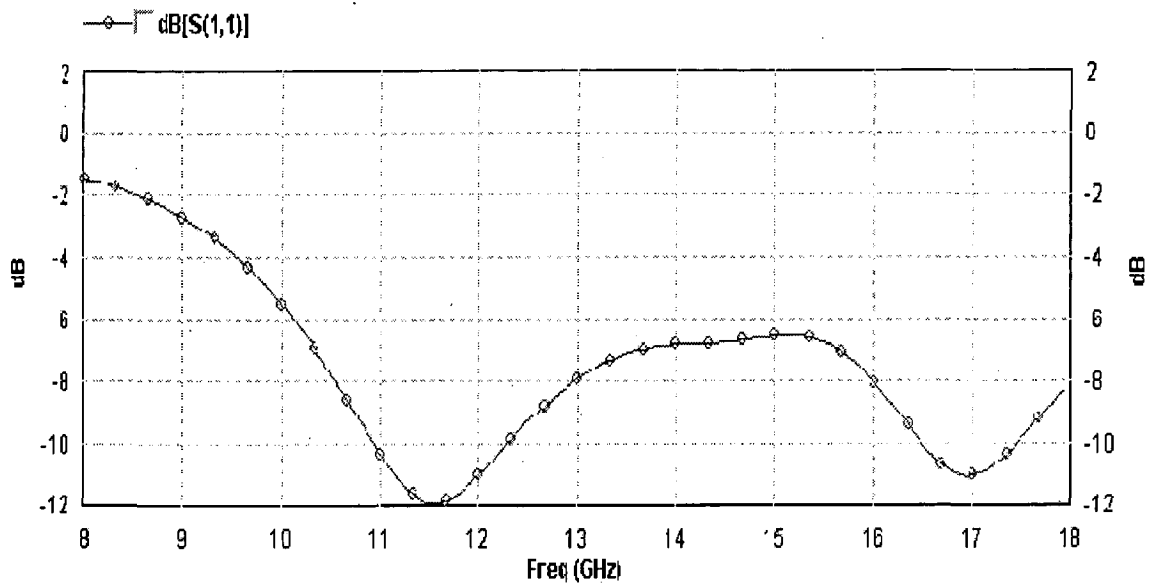


**Fig: 4.2** Simulated return loss dual patch MSA

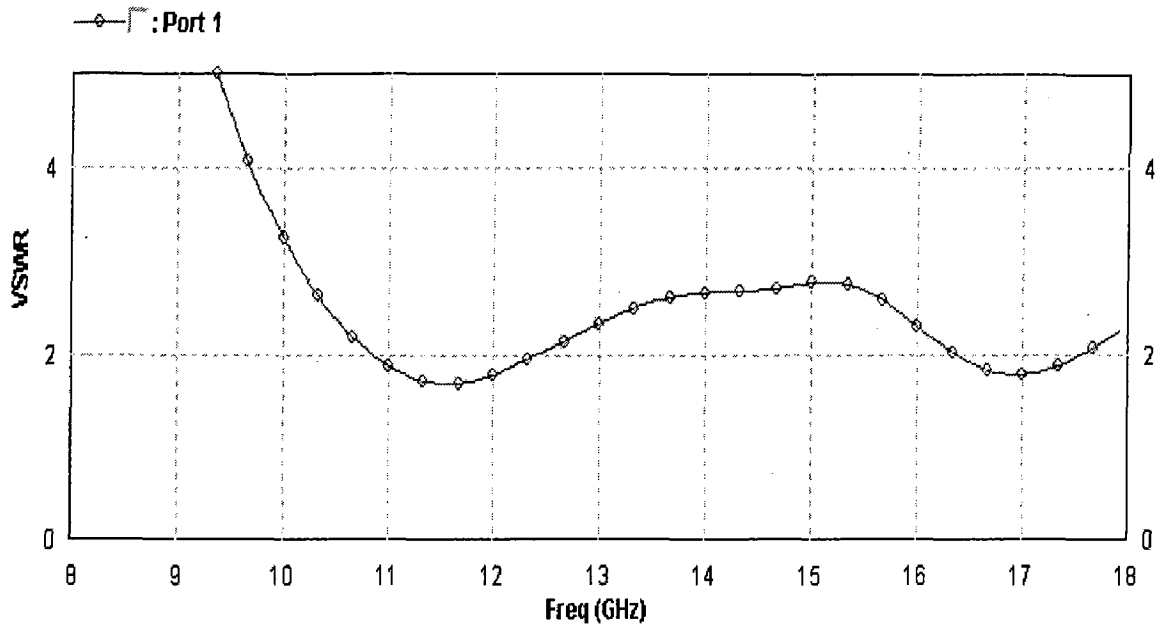
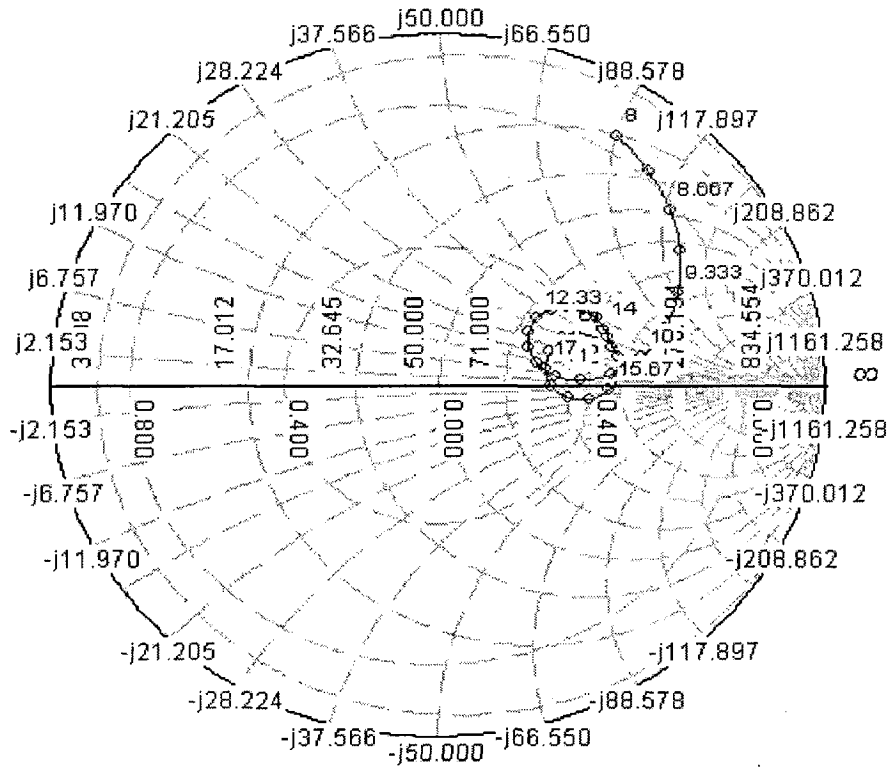


**Fig: 4.3 Simulated VSWR**



**Smith-Chart Display**

**Fig: 4.4 simulated smith chart**

### 4.3 ANN Implementation

The use of NN technique for antennas is not new and applications have been reported since 1990. In most of the applications, the role of the network is to form a black-box mapping between a set of input parameters with their corresponding responses. Some characteristics of the NN have been exploited here to locate the operational frequencies of the stacked microstrip antenna for specific design parameters.

#### 4.3.1 Data Generation

For generation of training data the parameter values was varied around the initial values. IE3D simulations were performed for these values and the operating frequencies were noted down. While data generation, it was kept in mind to take the dielectric constant of the lower laminate a higher value than that of the upper laminate and the relative dielectric constant of the upper laminate close to unity to give the best impedance bandwidth without compromising the antenna efficiency [11]. During simulation, these input data sets were discarded for which the operating frequencies fall beyond X/ Ku band.

#### 4.3.2 ANN Model

A multilayer perceptron trained in the back propagation mode [21] was used, because these networks are more effective in solving function mapping problems. The input and output of the NN is shown in Fig 4.5. In the present work  $\epsilon_{r3}$  and  $h_3$  were not taken as the input variables, because, the major role of the top layer is to provide a protection to the upper patch. Therefore in all the simulations  $\epsilon_{r3} = 2.2$  and  $h_3 = 3.09$  were taken as fixed values. The developed trained network parameters are given in Table-4.1. As the training progresses, the mean square error between the desired and the neural network output decreases, gradually updating the connecting weights of the neural network to an optimized value. The training curve is shown in Fig. 4.6.

In the model testing stage, a new set of input-output samples have been generated again using the IE3D simulation package. These are called testing data, which are used to test the accuracy of the network. The ability of neural model to predict accurate output when presented with input parameter values. A trained and tested neural model will be used online during the design stage, providing fast model evaluation. Training an MLP neural network with the use of back propagation algorithm to analysis the dual patch Microstrip antenna involves presenting

training data with input and output parameters. Differences between the desired outputs and the ANN outputs of the MLP-ANN are trained through the back propagation algorithm to adapt their weight parameters. During the training, the neural network performance is evaluated by computing difference between actual neural network outputs and desired outputs for all training samples. The difference is known as training or testing error. The weight parameters are adjusted during back propagation training, in such a way to minimize the error. The neural network training is carried out after the presentation of each training sample until the calculation accuracy of the network converged according to root mean square error function. The average training and testing error shown in the table 4.1.

Since the MLP neural model has been fully trained, it can learn from generalized patterns from given data and to model nonlinear relationship. Analysis has been carried out using different patch dimensions and other parameters of the dual patch MSAs to investigate their 1<sup>st</sup> and 2<sup>nd</sup> resonance frequencies using IE3D simulation packages.

Table 4.2 compares the 1<sup>st</sup> and 2<sup>nd</sup> resonance frequencies for EM-ANN model, EM simulation using IE3D simulation packages. Good accuracy was achieved by the EM-ANN model when compared with EM simulation. Using EM-ANN for dual patch microstrip antenna provides EM analysis capabilities. Analysis time for the patch antenna was under 1 minute. This confirms that substantial savings to computer time.

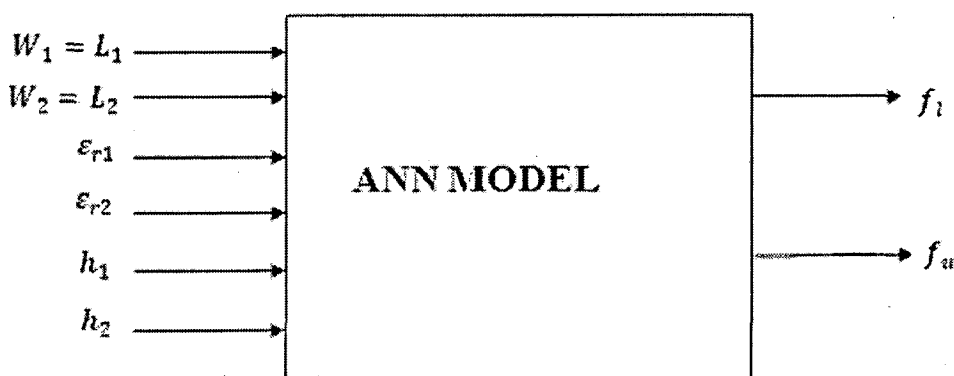


**Fig: 4.5** Analysis of the Dual Patch Microstrip Antenna Using ANN

**Table 4.1:**  
**Parameters of the developed neural network model for analysis**

Parameter	Value
No. of input neurons	6 (Dimensions of upper and lower patch, Height of upper and lower patch, Dielectric constant of upper and lower patch)
No. of output neurons	2 (Upper resonant and Lower resonant frequency)
No. of hidden neurons	25
Size of training data	115
Average training error	0.0167
Average testing error	0.0126
Learning rate	0.01
Numbers of epoches	200
Training algorithm	Backpropagation

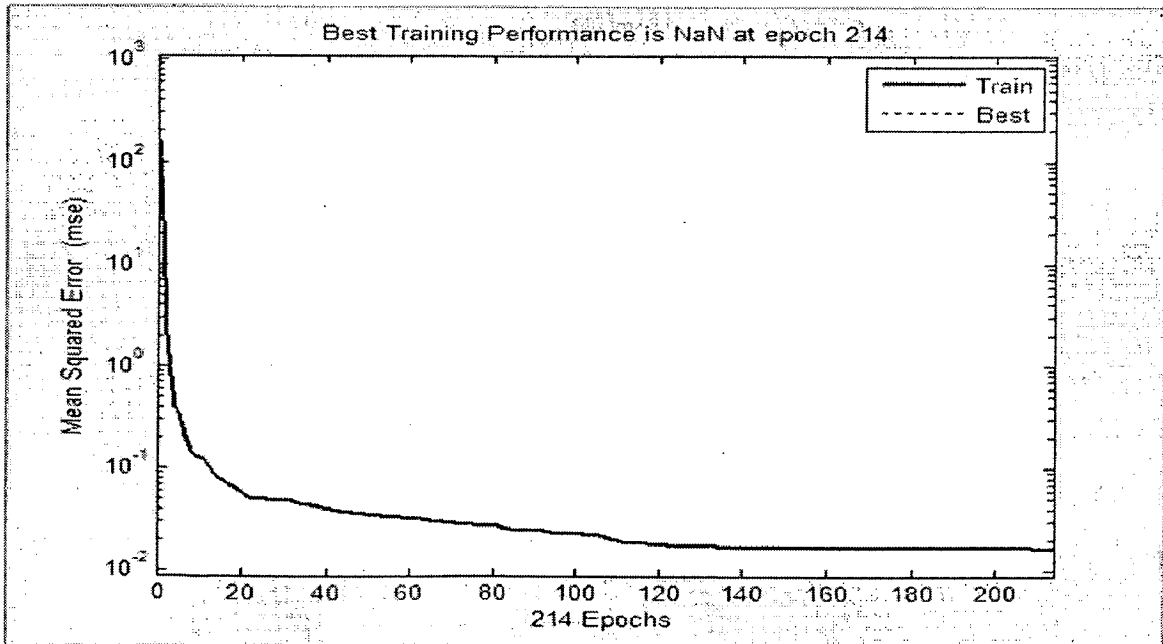


**Fig: 4.6 Mean Square Error Analysis Problem**



Table: 4.2

Resonant Frequency of Neural Network Model for few Training Data Set

Input Variables								Target(IE3D) GHz		ANN Response GHz	
W1 (mm)	L1 (mm)	H1 (mm)	$\epsilon_{r1}$	W2 (mm)	L2 (mm)	H2 (mm)	$\epsilon_{r2}$	$f_l$	$f_u$	$f_l$	$f_u$
7.5	7.5	1.53	2.2	6.9	6.9	1.53	1	11.9333	17.8667	12.0394	17.7649
8	8	1.53	2.2	6.9	6.9	1.53	1	11.5333	16.9333	11.5504	16.8944
8.2	8.2	1.53	2.2	6.9	6.9	1.53	1	11.3333	16.5333	11.3390	16.5205
8.5	8.5	1.53	2.2	6.9	6.9	1.53	1	11	15.9333	11.0095	15.9444
8.8	8.8	1.53	2.2	6.9	6.9	1.53	1	10.6667	15.4	10.6712	15.3689
9	9	1.53	2.2	6.9	6.9	1.53	1	10.4666	15	10.4449	15.0003
9.5	9.5	1.53	2.2	6.9	6.9	1.53	1	9.86666	14.2	9.89164	14.2164
10	10	1.53	2.2	6.9	6.9	1.53	1	9.4	13.4667	9.40692	13.4395
11	11	1.53	2.2	6.9	6.9	1.53	1	8.4	12.2	8.40091	12.1973
8	8	1	2.2	6.9	6.9	1.53	1	12	17.2	11.9899	17.2648
8	8	1.2	2.2	6.9	6.9	1.53	1	11.8667	17.1333	11.7999	17.0917
8	8	1.35	2.2	6.9	6.9	1.53	1	11.7333	17.0667	11.6832	16.9975
8	8	1.7	2.2	6.9	6.9	1.53	1	11.4	16.8	11.4202	16.7912
8	8	2	2.2	6.9	6.9	1.53	1	11.2	16.6	11.1685	16.5894
8	8	3	2.2	6.9	6.9	1.53	1	10.4667	15.9333	10.4665	15.9335
8	8	1.53	1	6.9	6.9	1.53	1	12.3333	17.9333	12.3426	17.9169
8	8	1.53	1.93	6.9	6.9	1.53	1	11.8667	16.4	11.8885	17.3883
8	8	1.53	2.25	6.9	6.9	1.53	1	11.4	16.7333	11.4776	16.7835
8	8	1.53	5.75	6.9	6.9	1.53	1	11.0667	16.2	11.0666	16.2000
8	8	1.53	13.1	6.9	6.9	1.53	1	8.86667	10.9333	8.84856	10.9348
8	8	1.53	2.2	6	6	1.53	1	12.0667	17.2667	12.0676	17.3177
8	8	1.53	2.2	7.4	7.4	1.53	1	11.0667	16.4667	11.1022	16.4716
8	8	1.53	2.2	9	9	1.53	1	9.66667	14.4667	9.66616	14.4665
8	8	1.53	2.2	6.9	6.9	1	1	11.6	16.8667	11.5873	16.9136

8	8	1.53	2.2	6.9	6.9	1.8	1	11.6	17.0667	11.5443	17.0150
8	8	1.53	2.2	6.9	6.9	3	1	13.3333	17.6	13.3273	17.5995
8	8	1.53	2.2	6.9	6.9	1.53	1.22	11.4667	16.6667	11.4605	16.6784

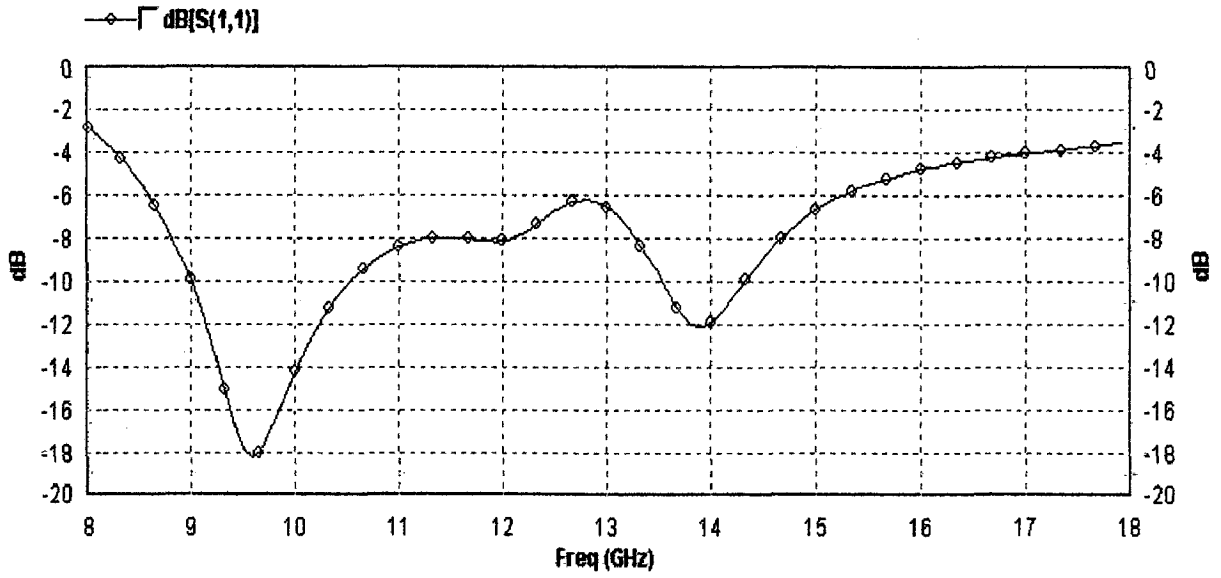
#### 4.4 Results and Discussion

The validity of the trained neural network was tested with the test data set that was not used for training purpose. The neural network response was compared with the simulations results from IE3D. Both these values along with return loss ( $S_{11}$ ) plot are shown in Fig.3. The accuracy of the network can be marked from these values. The response of the network was also tested with some typical experimental results and is shown in Fig: 4. Comparative study of the resonant frequency between simulated, ANN and experimental results for a test data set shown in table 4.3.

**Table 4.3**

**Resonant Frequency of Neural Network Model for Test Data Set**

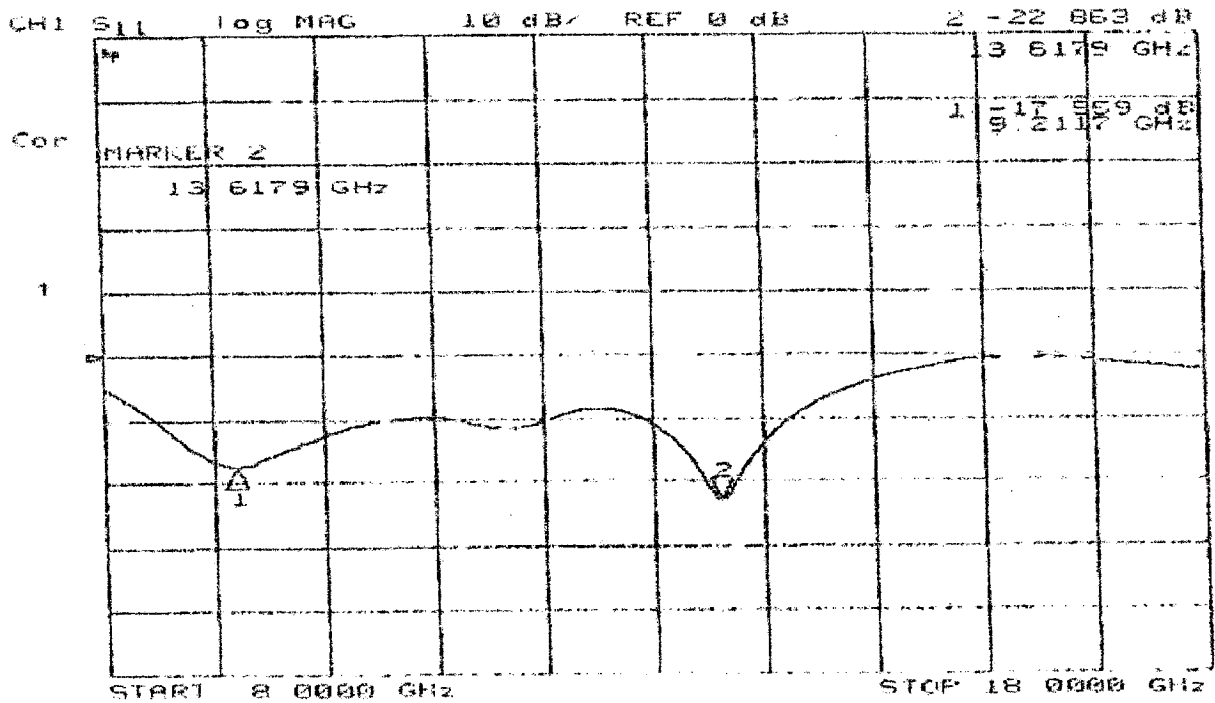
Input Variable						Simulated response (GHz)		ANN Response (GHz)		Experimental Response (GHz)	
$W_1$ (mm)	$h_1$ (mm)	$\epsilon_{r1}$	$W_2$ (mm)	$h_2$ (mm)	$\epsilon_{r2}$	$f_l$	$f_u$	$f_l$	$f_u$	$f_l$	$f_u$
8	1.5	2.5	6.9	2.1	1.2	10.8	15.8666	10.6852	15.8109	10.5620	14.048
8	1.5	3.2	6.9	2.1	1.2	9.8667	14.4	9.8668	14.5590	9.3564	13.7618
8	1.5	3.38	6.9	2.1	1.2	9.6667	14.0667	9.7255	14.3354	9.1709	13.5569
9	1.5	3.2	7.5	2.1	1.2	8.6667	12.5334	9.1214	13.4892	9.1910	12.9220
9	1.5	3.38	7.5	2.1	1.2	8.4667	12.2667	9.0486	13.3741	8.1218	11.8292



For  $W1=L1=8\text{mm}, \epsilon_{r1} = 2.5, h_1=1.5\text{mm}, W2=L2=6.9, \epsilon_{r2} = 1.2, h_2=2.1\text{mm}.$

$f_1= 9.6 \text{ GHz } f_2= 13.9334\text{GHz}$

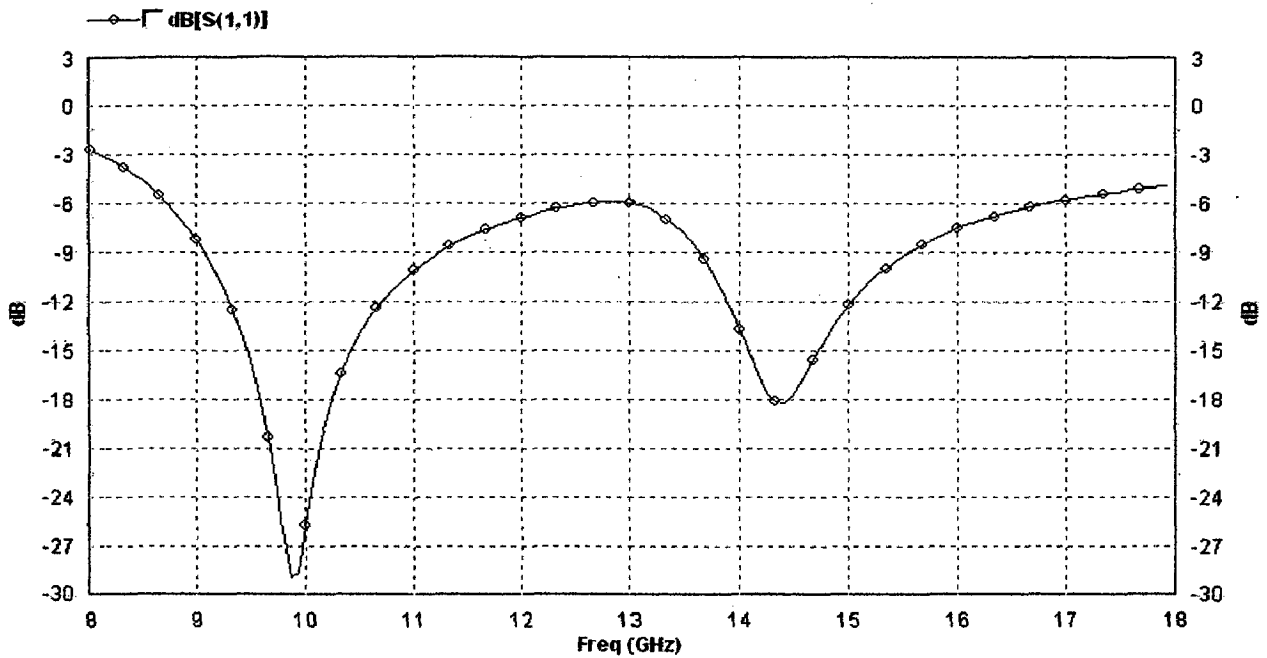
**Fig: 4.1 Simulated Return loss verses frequency**



$W1=L1=8\text{mm}, \epsilon_{r1} = 2.5, h_1=1.5\text{mm}, W2=L2=6.9, \epsilon_{r2} = 1.2, h_2=2.1\text{mm}$

$f_1= 9.2117\text{GHz}, f_2= 13.617 \text{ GHz}$

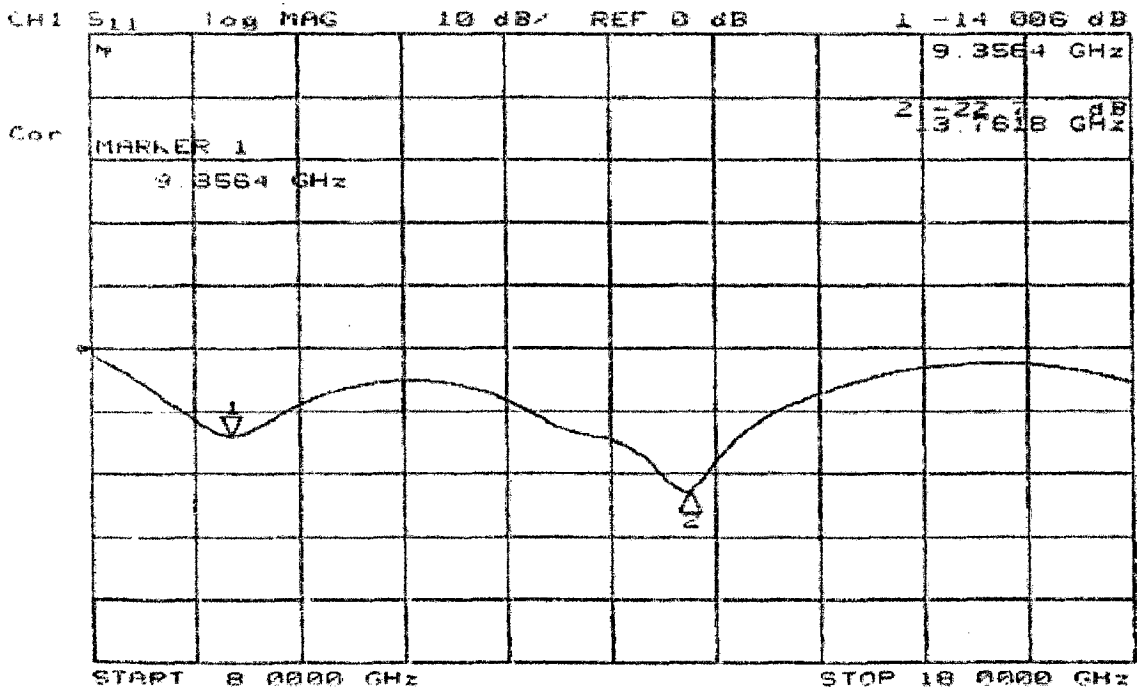
**Fig: 4.2 Experimental Return loss verses frequency**



For  $W1=L1=8\text{mm}, \epsilon_{r1} = 3.2, h_1=1.5\text{mm}, W2=L2=6.9, \epsilon_{r2} = 1.2, h_2=2.1\text{mm}.$

$f_1=9.8667\text{GHz}, f_2=14.4\text{ GHz}$

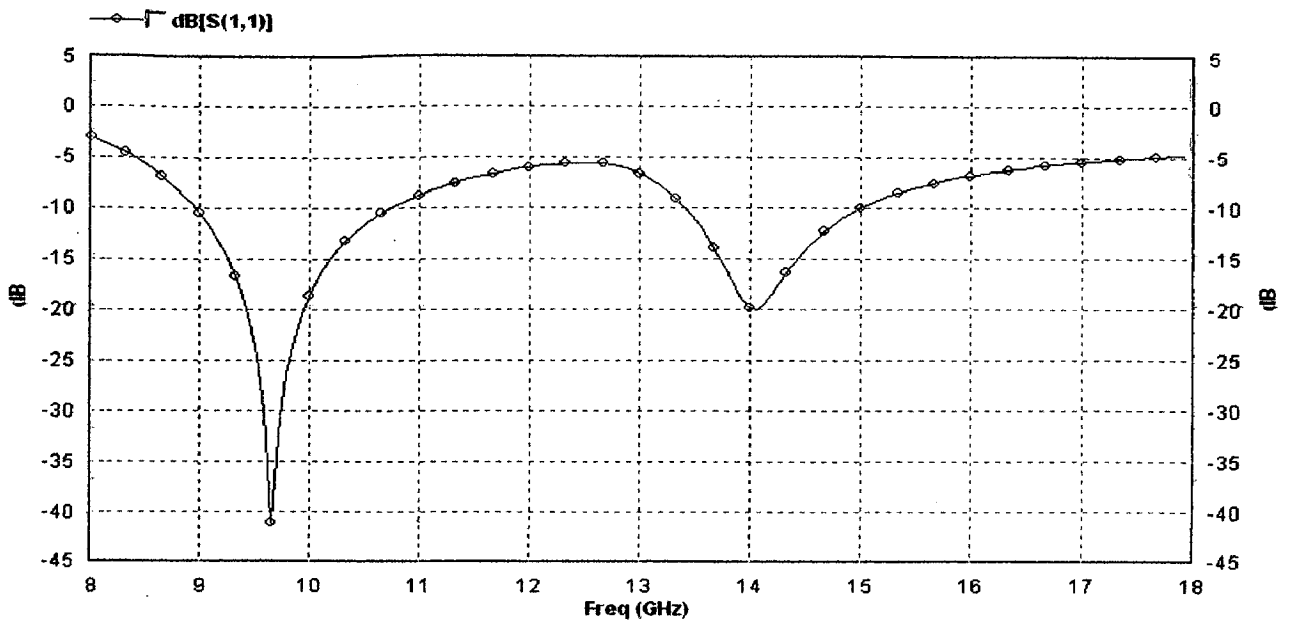
**Fig: 4.3 Simulated Return loss verses frequency**



$W1=L1=8\text{mm}, \epsilon_{r1} = 3.2, h_1=1.5\text{mm}, W2=L2=6.9, \epsilon_{r2} = 1.2, h_2=2.1\text{mm}$

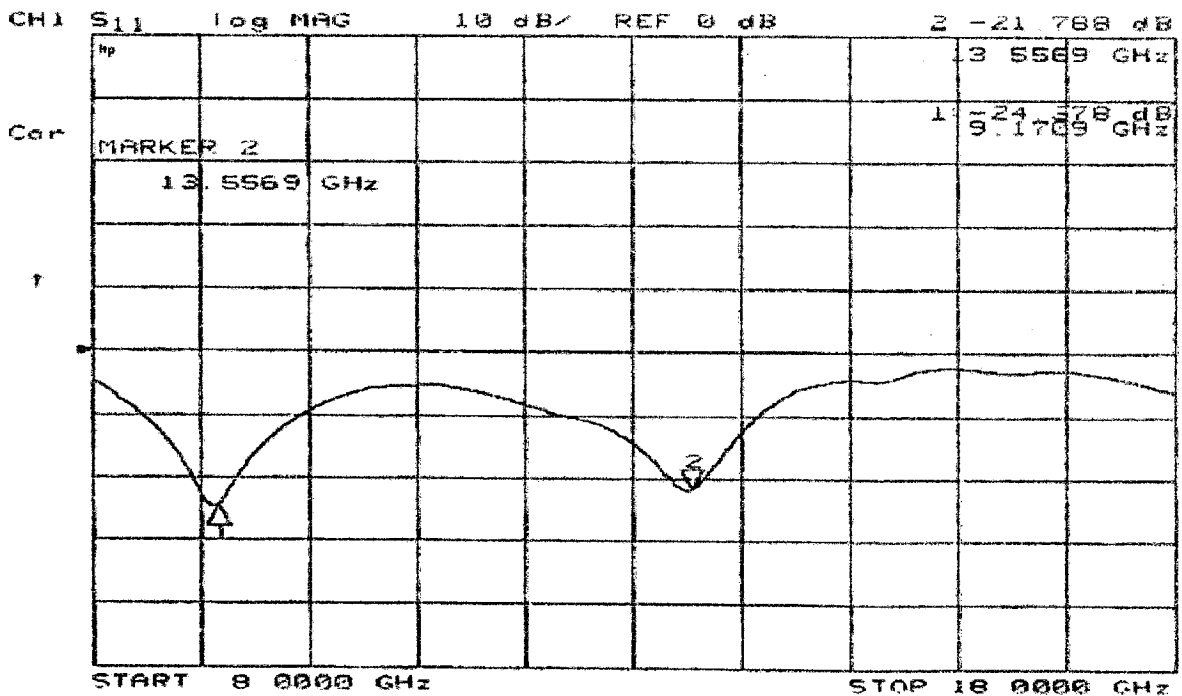
$f_1=9.3564\text{ GHz} f_2=13.76\text{GHz}$

**Fig: 4.4 Experimental Return loss verses frequency**



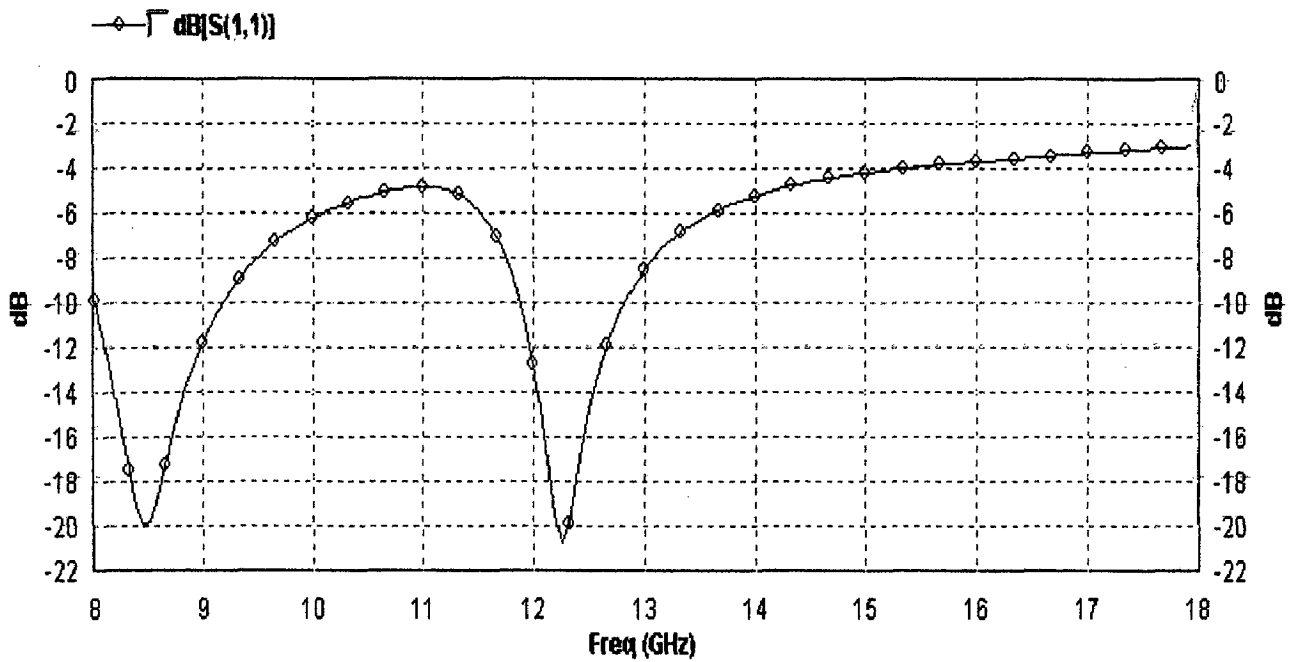
For  $W1=L1=8\text{mm}$ ,  $\epsilon_{r1} = 3.38$ ,  $h_1=1.5\text{mm}$ ,  $W2=L2=6.9$ ,  $\epsilon_{r2} = 1.2$ ,  $h_2=2.1\text{mm}$ .  
 $f_1=9.6667\text{ GHz}$   $f_2=14.0667\text{ GHz}$

Fig: 4.5 Simulated Return loss versus frequency



$W1=L1=8\text{mm}$ ,  $\epsilon_{r1} = 3.38$ ,  $h_1=1.5\text{mm}$ ,  $W2=L2=6.9$ ,  $\epsilon_{r2} = 1.2$ ,  $h_2=2.1\text{mm}$ .  
 $f_1= 9.1709\text{GHz}$   $f_2=13.5569\text{ GHz}$

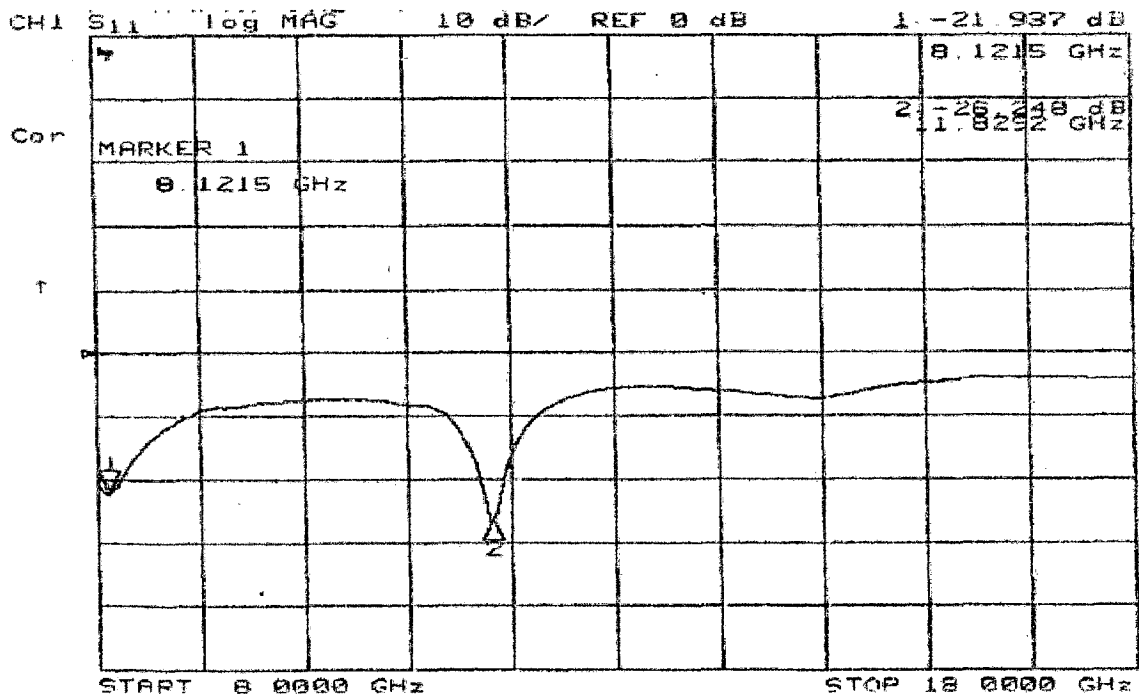
Fig: 4.6 Experimental Return loss versus frequency



For  $W1=L1=9\text{mm}$ ,  $\epsilon_{r1} = 3.38$ ,  $h_1=1.5\text{mm}$ ,  $W2=L2=7.5$ ,  $\epsilon_{r2} = 1.2$ ,  $h_2=2.1\text{mm}$ .

$f_1=8.4667$  GHz,  $f_2=12.2667$  GHz

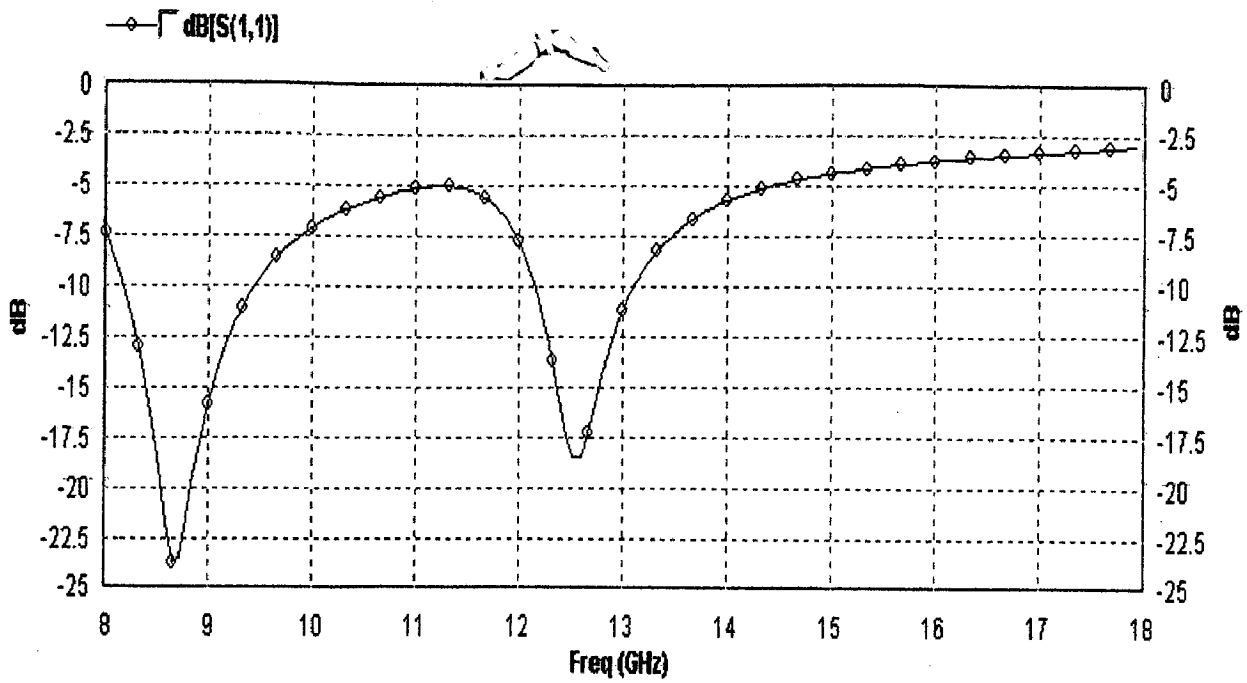
Fig: 4.9 Simulated Return loss versus frequency



$W1=L1=9\text{mm}$ ,  $\epsilon_{r1} = 3.38$ ,  $h_1=1.5\text{mm}$ ,  $W2=L2=7.5$ ,  $\epsilon_{r2} = 1.2$ ,  $h_2=2.1\text{mm}$

$f_1= 8.1215\text{GHz}$ ,  $f_2=11.8292$  GHz

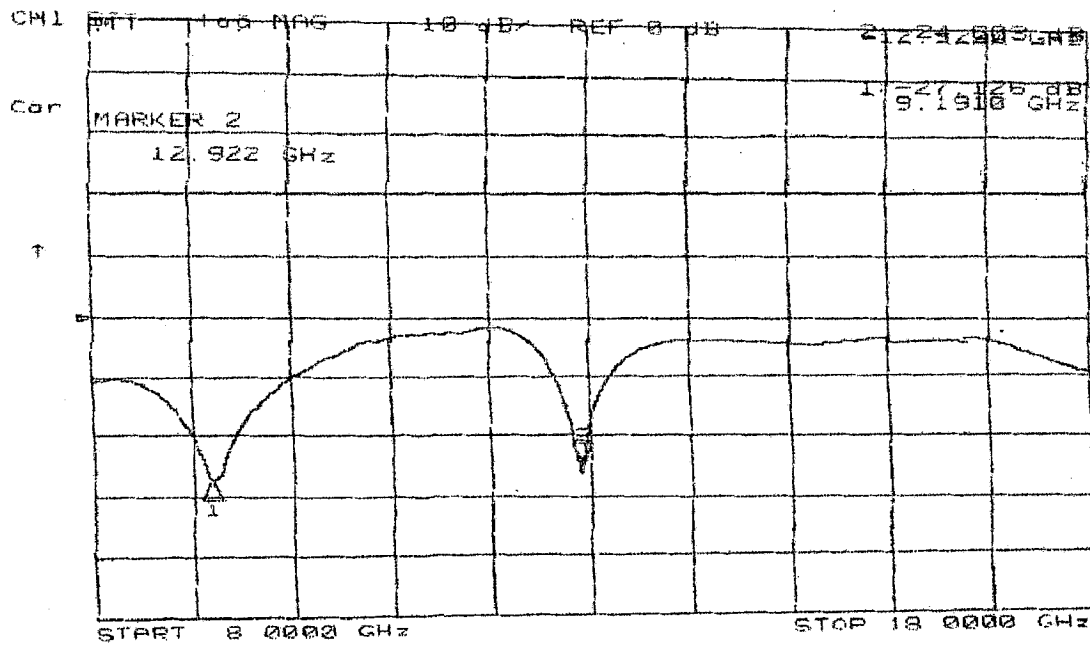
Fig 6.10 Experimental Return loss versus frequency



For  $W1=L1=9\text{mm}, \epsilon_{r1} = 3.2, h_1=1.5\text{mm}, W2=L2=7.5, \epsilon_{r2} = 1.2, h_2=2.1\text{mm}.$

$f_1 = 8.667\text{GHz}$   $f_2 = 12.5334\text{GHz}$

**Fig: 4.7** Simulated Return loss verses frequency



$W1=L1=9\text{mm}, \epsilon_{r1} = 3.2, h_1=1.5\text{mm}, W2=L2=7.5, \epsilon_{r2} = 1.2, h_2=2.1\text{mm}$

$f_1 = 9.1910\text{GHz}$ ,  $f_2 = 12.922\text{GHz}$

**Fig: 4.8** Experimental Return loss verses frequency

## **Design of Stacked Microstrip Antenna**

---

### **5.1 Introduction**

This chapter deals in finding the dimensions of the patches for the stacked microstrip antenna to resonate at desired frequencies, using neural network technique. Usually in microstrip antenna design ' $\epsilon_r$ ' and ' $h$ ' is given, and the user is asked to design the antenna for a specific frequency. So, the developed neural network takes the desired lower and upper resonant frequency of a dual patch stacked microstrip antenna along with heights and dielectric constants of both the layers as input and delivers the dimensions of the two patches as output. The validity of the network is tested with simulations from IE3D as well as with experimental results. The following section describes the neural network implementation process followed by the results obtained.

### **5.2 ANN Implementation**

Neural network techniques have already been approached for design of single layer patch antennas. But for stacked patch antennas, as the number of parameters for the design of the antenna increases, so neural network is a suitable candidate to handle the problem. The approach followed in case of design is same as that followed in analysis case, but the only difference is the input/output parameters.

#### **5.2.1 Data Generation**

The same data set used for analysis was used for design also, with some rearrangements. The output parameters in this case are the dimensions of the two stacked patches.

#### **5.2.2 ANN Model**

Multilayer Perceptron trained in the backpropagation mode is used in this case also to form the black-box modeling between the input-output parameters. The network parameters are shown in Table. 5.1 And the training curve is shown in Fig.5.1.



The proposed method involves training the neural network to design the patch antenna when the patch sizes, height of the both dielectric layers and their dielectric constants and upper and lower patch resonance frequencies are given as  $(f_u, f_l)$ . The input vectors to the neural network model are the upper and lower patch resonant frequency, height of both upper and lower patches and dielectric constants of the upper and lower patch. The output values are dimensions of the upper and lower patches ( $W_1=L_1, W_2=L_2$ ) to the MLP-NN. A simultaneous training and testing methodology is used while training the MLP-NN model. The MLP-NN model contains a three layer of nodes, first input layer, where input to the network are applied, second is the output layer, where the output of the network are produced and one or more layers of nodes in between the input and output layer, referred to as hidden layer. The type of connections allowed in the MLP trained with the backpropagation algorithm is feed forward types of connections. The simulated data set is separated into sets: one is for training and other one for simultaneous testing and model verification. In this way, testing set errors can be monitored as training progress. When the testing error increases, the training is stopped, preventing over-fitting of the training data.

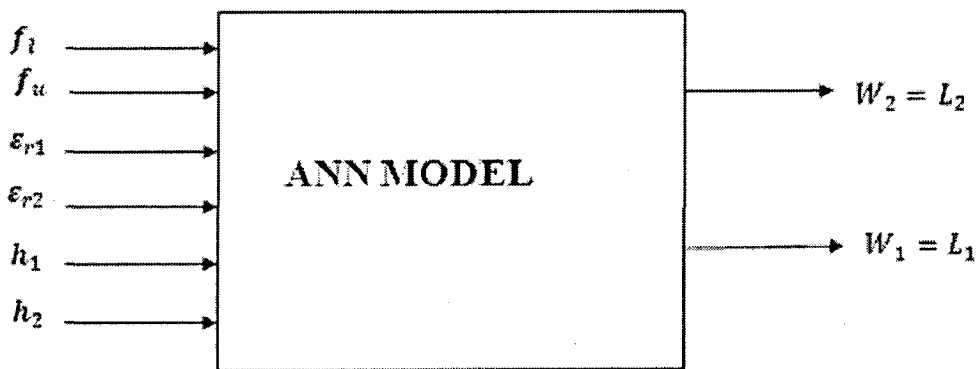


**Fig: 5.1** Design of the Dual Patch Microstrip Antenna Using ANN

**Table 5.1**

**Parameters of the developed neural network model for design**

Parameter	Value
No. of input neurons	6 (Upper resonance and Lower resonance frequency, Height of upper and lower patch, Dielectric constant of upper and lower patch)
No. of output neurons	2 (Dimensions of upper and lower patch)
No. of hidden neurons	25
Size of training data	115
Average training error	0.0000148
Average testing error	0.00000070724
Learning rate	0.1
Numbers of epochs	1000
Training algorithm	Backpropagation

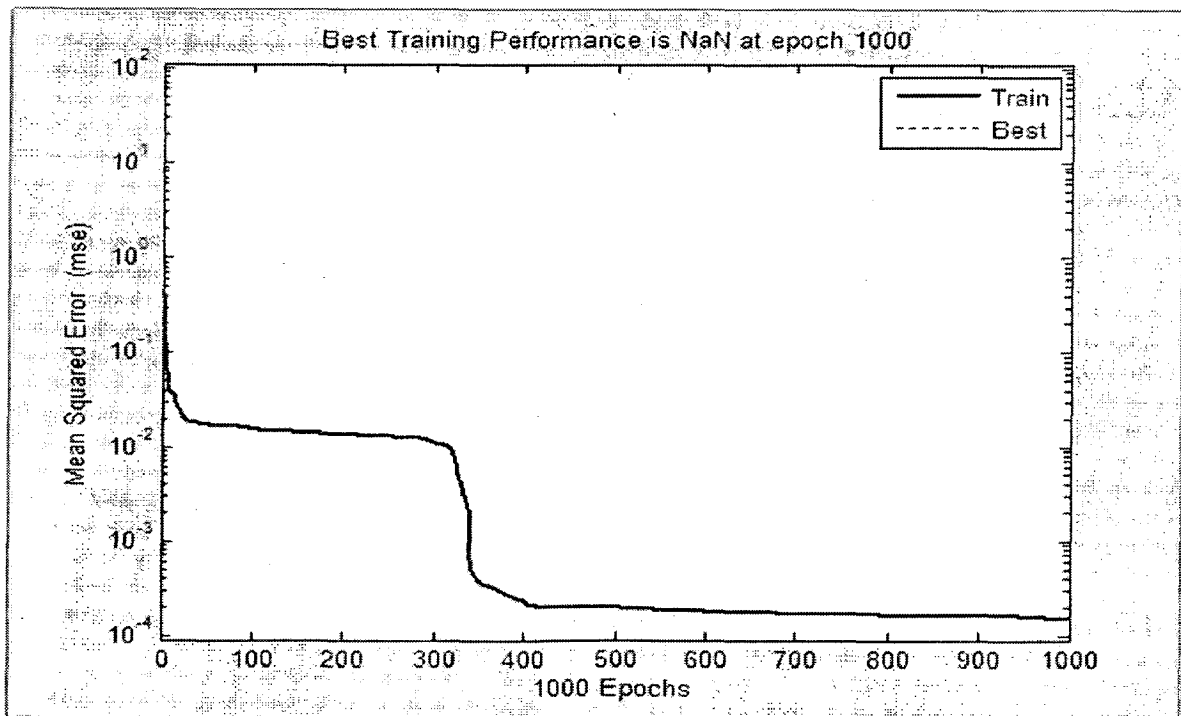


**Fig: 5.2 Mean Square Error Design Problem**

**Table 5.2**

**Patch Dimensions of neural network model for few training data set**

Input Variables						Dimension(IE3D)		ANN Response	
$f_l$	$f_u$	$\epsilon_{r1}$	$h_1$	$h_2$	$\epsilon_{r1}$	W1	W2	W1	W2
(GHz)	(GHz)		(mm)	(mm)		(mm)	(mm)	(mm)	(mm)
11.9333	17.8667	2.2	1.53	1.53	1	7.5	6.9	7.5025	6.9023
11.5333	16.9333	2.2	1.53	1.53	1	8	6.9	7.9972	6.9025
11.3333	16.5333	2.2	1.53	1.53	1	8.2	6.9	8.1422	6.9058
11	15.9333	2.2	1.53	1.53	1	8.5	6.9	8.4855	6.9032
10.6667	15.4	2.2	1.53	1.53	1	8.8	6.9	8.7956	6.8969
10.4666	15	2.2	1.53	1.53	1	9	6.9	9.0020	6.9006
9.8666	14.2	2.2	1.53	1.53	1	9.5	6.9	9.5064	6.9052
9.4	13.4667	2.2	1.53	1.53	1	10	6.9	10.0005	6.8957
8.4	12.2	2.2	1.53	1.53	1	11	6.9	10.9998	6.9002
12	17.2	2.2	1	1.53	1	8	6.9	8.0083	6.9059
11.8667	17.1333	2.2	1.2	1.53	1	8	6.9	8.0061	6.8853
11.7333	17.0667	2.2	1.35	1.53	1	8	6.9	7.9971	6.9079
11.4	16.8	2.2	1.7	1.53	1	8	6.9	7.9925	6.9038
11.2	16.6	2.2	2	1.53	1	8	6.9	7.9990	6.8988
10.4667	15.9333	2.2	3	1.53	1	8	6.9	8.0002	6.9000
12.3333	17.9333	1	1.53	1.53	1	8	6.9	7.9998	6.9002
11.8667	16.4	1.93	1.53	1.53	1	8	6.9	8.0023	6.9006
11.4	16.7333	2.25	1.53	1.53	1	8	6.9	8.0105	6.9032
11.0667	16.2	5.75	1.53	1.53	1	8	6.9	8.0000	6.9000
8.86667	10.9333	13.1	1.53	1.53	1	8	6.9	8.0011	6.8986
12.0667	17.2667	2.2	1.53	1.53	1	8	6	8.0109	6.0089
11.0667	16.4667	2.2	1.53	1.53	1	8	7.4	8.0030	7.4248
9.6666	14.4667	2.2	1.53	1.53	1	8	9	8.0006	9.0011
11.6	16.8667	2.2	1.53	1	1	8	6.9	7.9990	6.8997

11.6	17.0667	2.2	1.53	1.8	1	8	6.9	8.0032	6.9038
13.3333	17.6	2.2	1.53	3	1	8	6.9	8.0011	6.9003
11.4667	16.6667	2.2	1.53	1.53	1.22	8	6.9	8.0063	6.9053
10.3333	17.4667	2.2	1.53	1.53	2.1	8	6.9	7.9954	6.9033

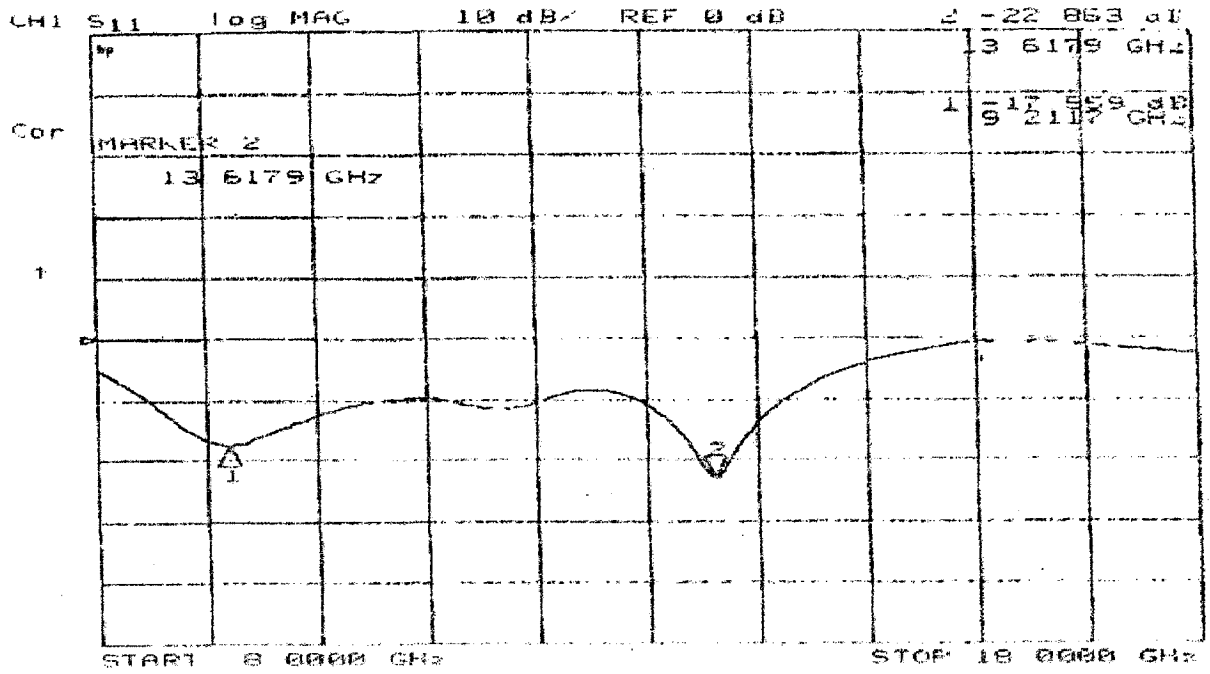
### 5.3 Results and Discussion

In this case also, the validity of the trained neural network was tested with the test data set that was not used for training purpose. The neural network response was compared with the simulations results from IE3D. The comparison values are shown in Table.5.2. The accuracy of the network can be marked from these values. The response of the network was also tested with some typical experimental results table 5.3 and is shown in Fig. 5.

**Table 5.3**

**Patch Dimensions of neural network model for test data set**

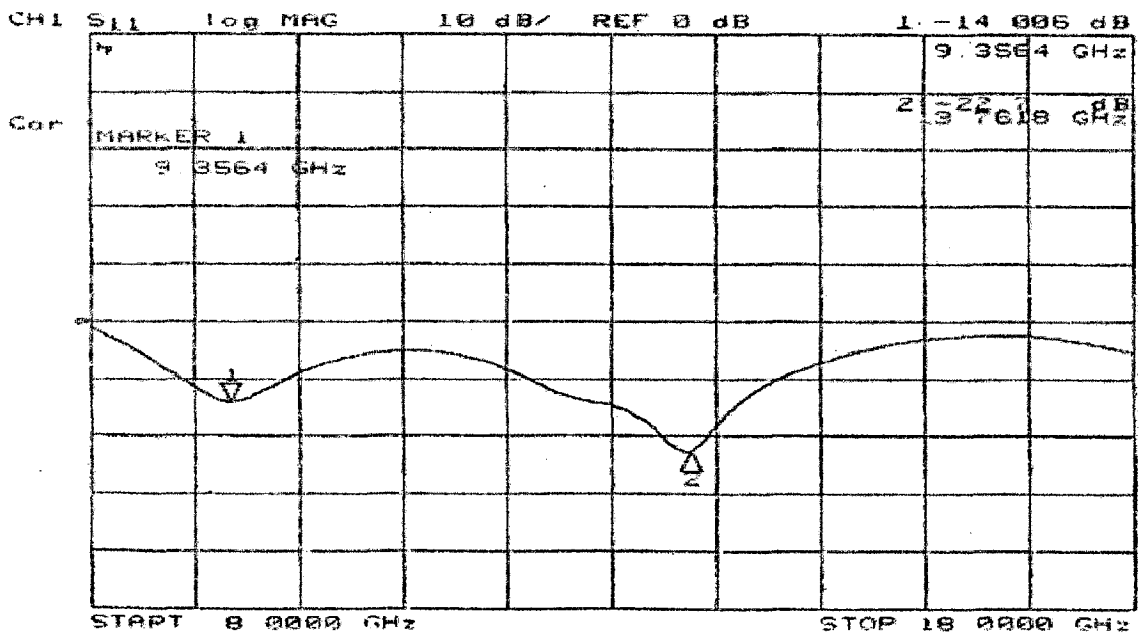
Input Variables						Dimension(IE3D)		ANN Response	
$f_l$ (GHz)	$f_u$ (GHz)	$\epsilon_{r1}$	$h_1$ (mm)	$h_2$ (mm)	$\epsilon_{r2}$	W1 (mm)	W2 (mm)	W1 (mm)	W2 (mm)
10.5620	14.048	2.5	1.5	2.1	1.2	8	6.9	8.1186	6.7512
9.3564	13.7618	3.2	1.5	2.1	1.2	8	6.9	8.1578	6.7216
9.1709	13.5569	3.38	1.5	2.1	1.2	8	6.9	8.1134	6.7832
9.1910	12.9220	3.2	1.5	2.1	1.2	9	7.5	9.1125	7.3502
8.1218	11.8292	3.38	1.5	2.1	1.2	9	7.5	9.2017	7.4552



$W1=L1=8\text{mm}, \epsilon_{r1} = 2.5, h_1=1.5\text{mm}, W2=L2=6.9, \epsilon_{r2} = 1.2, h_2=2.1\text{mm}$

$f_1=9.2117\text{GHz}, f_2=13.617\text{GHz}$

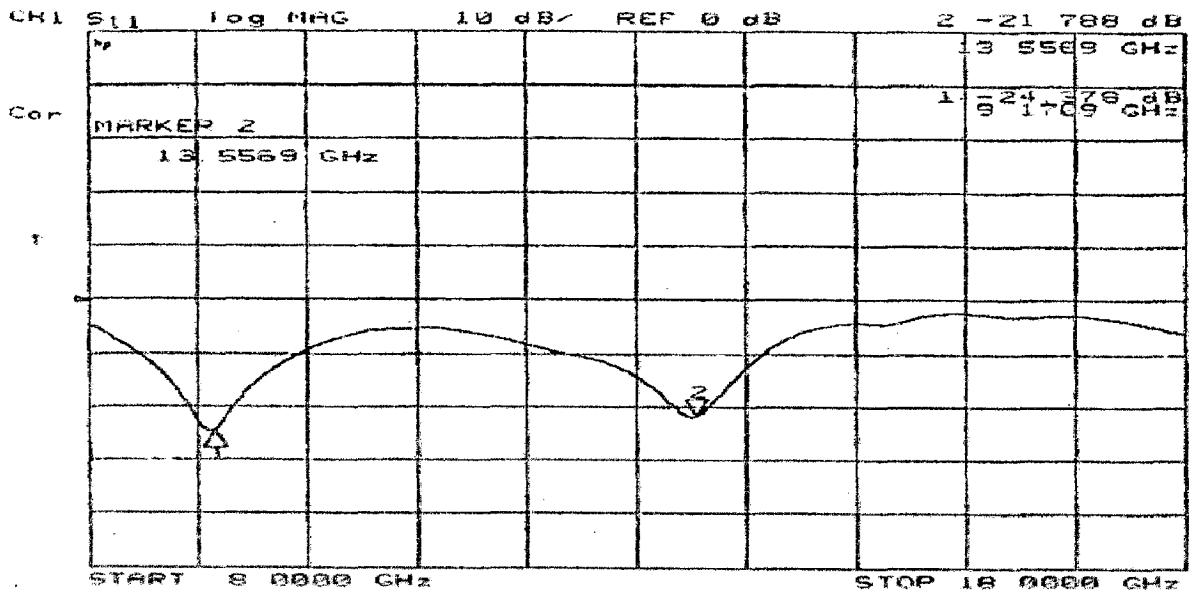
Fig: 5(a) Experimental Return loss verses frequency



$W1=L1=8\text{mm}, \epsilon_{r1} = 3.2, h_1=1.5\text{mm}, W2=L2=6.9, \epsilon_{r2} = 1.2, h_2=2.1\text{mm}$

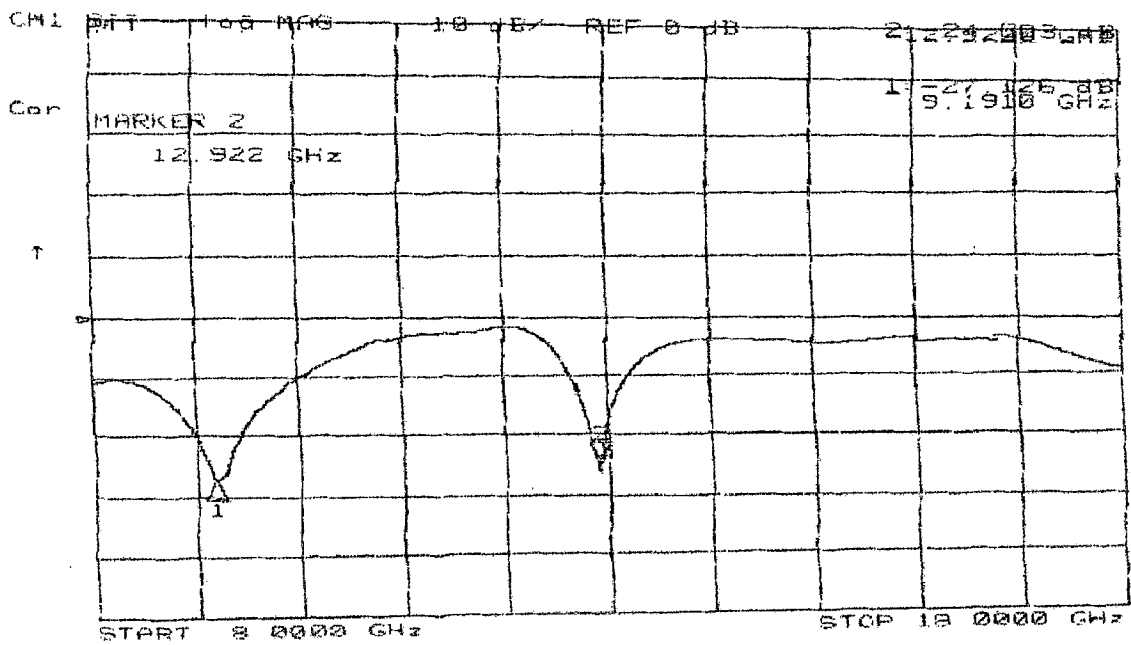
$f_1=9.3564\text{GHz}, f_2=13.76\text{GHz}$

Fig: 5(b) Experimental Return loss verses frequency



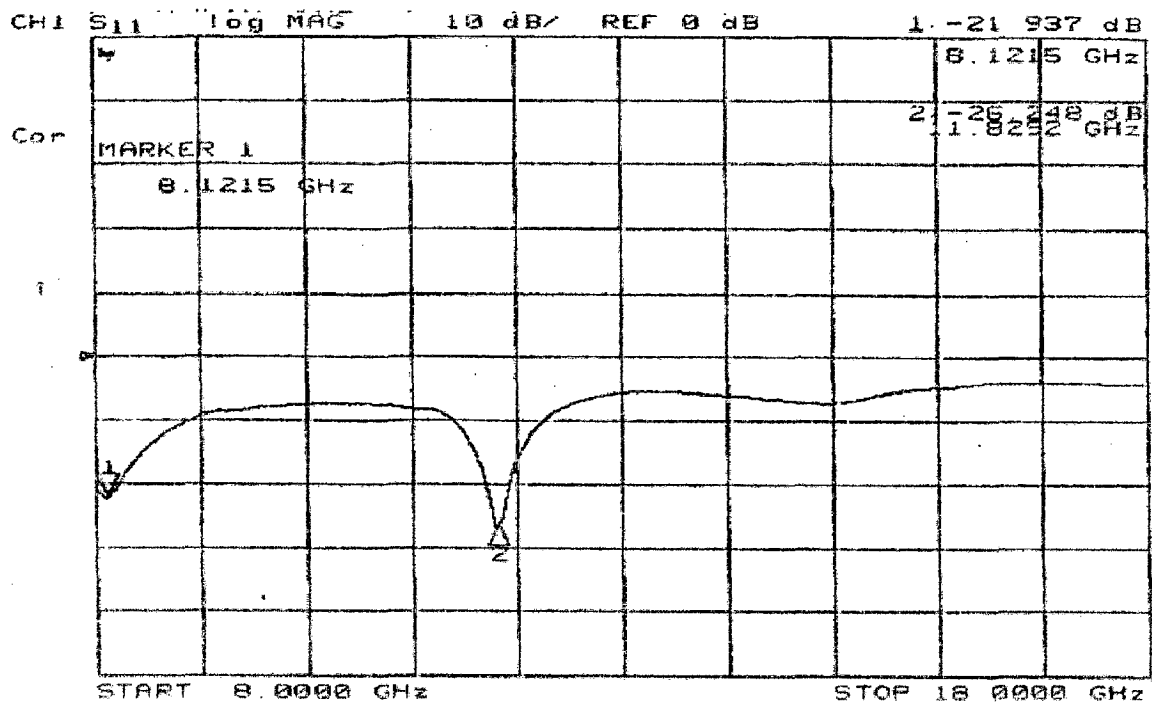
$W1=L1=8\text{mm}, \epsilon_{r1} = 3.38, h_1=1.5\text{mm}, W2=L2=6.9, \epsilon_{r2} = 1.2, h_2=2.1\text{mm}$   
 $f_1=9.1709\text{GHz} \quad f_2=13.5569\text{GHz}$

**Fig: 5(c)** Experimental Return loss verses frequency



$W1=L1=9\text{mm}, \epsilon_{r1} = 3.2, h_1=1.5\text{mm}, W2=L2=7.5, \epsilon_{r2} = 1.2, h_2=2.1\text{mm}$   
 $f_1=9.1910\text{GHz}, \quad f_2=12.922\text{GHz}$

**Fig: 5(d)** Experimental return loss verses frequency



$W1=L1=9\text{mm}, \epsilon_{r1} = 3.38, h_1=1.5\text{mm}, W2=L2=7.5, \epsilon_{r2} = 1.2, h_2=2.1\text{mm}$

$f_1= 8.1215\text{GHz}, f_2=11.8292 \text{GHz}$

**Fig: 5(e)** Experimental Return loss verses frequency

## **Conclusions and Scope for Future Work**

---

### **6.1 Conclusions**

A method based on neural networks is presented both for analysis and design of stacked microstrip antennas. In the model for analysis, the network gives the resonant frequencies of antenna as its response, where as in the design neural model, it gives the dimensions of the patches a dual patch microstrip antenna. Both the networks were trained using the well known backpropagation training algorithm. The validity of these networks was tested with the test data, i.e., the data that was not used for the training of the neural networks. The responses of the developed network were also compared with some typical experimental results. The results obtained from the developed networks are quite in agreement with the test data as well as experimental results, verifying the accuracy of the network model. Because the networks are robust both from the angle of accuracy and time of computation, therefore these models can be used as CAD models for analysis and design of stacked patch antennas, within the specified range of the parameters.

### **7. Scope for Future Work**

The generated benefit of using neural networks is its fast response time, besides accuracy. Therefore, in order to find optimized structures, instead of commercial software, the developed network can be used in conjunction with other biologically inspired optimization techniques like GA, PSO etc.

In the present work, we took more parameters are constants, like the permittivity and height of the protective layer, feed position etc. varying values of their parameters can also be considered while developing the trained networks in order to make it a more generated one.



## References

---

- [1] Deschamps, G. A., "Microstrip Microwave Antennas," *Proc. 3rd USAF Symposium on Antennas*, 1953.
- [2] Munson, R.E., "Conformal Microstrip Antennas and Microstrip Phased Arrays," *IEEE Trans. Antennas Propagation*, Vol. AP-22, pp. 74–78, 1974.
- [3] Howell, J. Q., "Microstrip Antennas," *IEEE Trans. Antennas Propagation*, Vol. AP-23, pp. 90–93, January 1975.
- [4] James, J. R., and P. S. Hall, *Handbook of Microstrip Antennas*, Vol. 1, London: Peter
- [5] Gupta, K. C, and A. Bennella, *Microstrip Antennas Theory and Design*, Norwood, MA: Artech House, 1988.
- [6] Pozar, D. M., and D. H. Schaubert, *Microstrip Antennas: The Analysis and Design of Microstrip Antennas and Arrays*, New York: IEEE Press, 1995.
- [7] Sainati, R. A., *CAD of Microstrip Antennas for Wireless Applications*, Norwood, MA: Artech House, 1996.
- [8] Lee, H. F., and W. Chen, *Advances in Microstrip and Printed Antennas*, New York: John Wiley & Sons, Inc., 1997.
- [9] Damiano, J. P., J. Bennegoueche, and A. Papiernik, "Study of Multilayer Antennas with Radiating Elements of Various Geometry," *Proc. IEE, Microwaves, Antennas Propagation*, Pt. H, Vol. 137, No. 3, 1990, pp. 163–170.
- [10] Sabban, A., "A New Broadband Stacked Two Layer Microstrip Antenna," *IEEE AP-S Int. Symp. Digest*, June 1983, pp. 63–66.
- [11] Girish kumar and Ray K.P., "*Broadband microstrip Antenna*", Artech House, 2002.
- [12] Bahl, I. J., and P. Bhartia, *Microstrip Antennas*, Dedham, MA: Artech House, 1980.
- [13] Splitt, G., and M. Davidovitz, "Guidelines for the Design of Electromagnetically Coupled Microstrip Patch Antennas on Two-Layered Substrate," *IEEE Trans. Antennas Propagation*, Vol. AP-38, No. 7, 1990, pp. 1136–1140.
- [14] Lee R.Q., Lee K.F., and Bobinchak J. "characteristics of two layer electromagnetically coupled rectangular patch antenna," *Electron. Letters*, Vol. 23, No. 20, pp. 1070-1072, 1987.

- [15] Carver, K. R., and J. W. Mink, "Microstrip Antenna Technology," *IEEE Transaction Antennas Propagation*, Vol. AP-29, pp. 2–24, January 1981.
- [16] Pozar, D. M., "Microstrip Antenna Aperture-Coupled to a Microstrip Line," *Electronics Letters*, Vol. 21, No. 2, pp. 49–50, 1985.
- [17] Targonski S. D., Waterhouse R. B., "Design of Wide-Band Aperture-Stacked Patch Microstrip Antennas" *IEEE Transactions on Antenna and Propagation*, VOL. 46, NO. 9, September 1998.
- [18] Pozar, D. M., and B. Kaufman, "Increasing the Bandwidth of a Microstrip Antenna by Proximity Coupling," *Electronics Letters*, Vol. 23, No. 8, pp. 368–371, 1987.
- [19] Crop F., Kossiavas G., papiernik A., "Stacked resonators for bandwidth enhancement a comparison of two feeding techniques," *IEE proceedings-H*, Vol. 140, no. 4, pp. 303-308, August 1993.
- [20] IE3D 9.0, Zeland Software Inc., Fremont, CA.
- [21] Haykin S., *Neural Networks: a Comprehensive Foundation*, Second edition, Prentice- Hall Inc., Boston, 1999.
- [22] Christodoulou, C. and M. Georgiopoulos, *Applications of Neural Networks in Electromagnetic*, Artech House, Boston, 2001.
- [23] Jacek M. Zurada , *Introduction to Artificial Neural Systems*, PWS Publishing Co. Boston, MA, USA.
- [24] Sagiroglu S., Guney K., "Calculation of resonant frequency for an equilateral triangular microstrip antennas with the use artificial neural networks", *Microwave and optical technology letters* Vol.14, No.2, February 1997.
- [25] Mishra R. K., Patnaik A., "Neural Network-based CAD Model for the Design of Square Patch Antennas," *IEEE Trans. on Antennas Propagations*, Vol. 46, No. 12, pp. 1890–1891, November 1998.
- [26] Sagiroglu S., Guney K., Erler M., "Resonant frequency calculation for circular microstrip antennas using artificial neural networks", *International Journal of RF and Microwave Computer-Aided Engineering*, Vol.8, No.3, pp. 270-277, 1998
- [27] Karaboga D., Sagiroglu S., Guney K., Erler M., "Neural computation of resonant frequency of electrically thin and thick rectangular microstrip antennas," *Microwave , Antenna and Propagation, IEEE Proceedings*, vol. 146, No. 3, pp. 155-159, April 1999.

- [28] Somasiri, N.P., Toh, W.K., Chen, X., Robertson, I.D., and Rezazadeh, A. A.: “Numerical modelling of multi-layered microstrip patch antennas”, *8<sup>th</sup> IEEE Int. Conf. on telecommunication*, Bucharest, Romania, June 2001.
- [29] Somasiri, N.P., Chen, X., Robertson, I.D., and Rezazadeh, A.A.: “Full wave analyses for a multi-layered microstrip patch antenna”, *Int. J. Infrared Millim. Waves*, Vol. 23, pp. 1777–1785, 2002.
- [30] Guney K., sagiroglu S., Erler M., “Generalised neural method to determine resonant frequencies of various microstrip antennas,” *Inc International Journal RF and microwave Computer-Aided Engineering*, Vol 12, pp. 131-139, Jan 2002.
- [31] Somasiri N.P., Chen X., Robertson, I.D. and Rezazadeh, A.A., “A neural Network modeller for multi-layered microstrip patches antennas,” *12th IEE Int. Conf. on Antennas and Propagation*, Exeter, UK, 31 April–3 May 2003.
- [32] Angiulli G., Versaci M., “Resonant frequency evaluation of microstrip antennas using a neural-fuzzy approach”, *IEEE Transactions Magnetics*, Vol. 39, No. 3, pp. 1333 – 1336, May 2003.
- [33] Guney K. and Gultekin S.S., “Artificial neural networks for resonant frequency calculation of rectangular microstrip antennas with thin and thick substrates,” *International journal of infrared and millimetre waves*, Vol. 25, No. 9, Sept. 2004.
- [34] Somasiri, N.P.; Chen, X.; Rezazadeh, A.A.; “Neural network modeller for design optimisation of multilayer patch antennas,” *IEEE Trans. Antennas Propag. Magazine*, Vol.151, pp: 514 – 518, Dec.2004.
- [35] Nurhan Turker, Filiz Gunes, Tulay Yildirim, “Artificial Neural Design of Microstrip Antenna,” *Turk J. Elec. Engineering*, Vol.14, No.3, pp 445-453, 2006.
- [36] Siakavara K., “Artificial Neural Network Employment in the Design of Multilayered Microstrip Antenna with Specified Frequency Operation,” *PIERS Proceedings, August 27-30, Prague, Czech Republic*, pp. 210-214,2007.
- [37] Moghaddasi M.N, Barjoei P.D., Naghsh A.,“A Heuristic Artificial Neural Network for Analyzing and synthesizing Rectangular Microstrip Antenna,” *IJCSNS International Journal of Computer Science and Network Security*, VOL.7 No.12, December 2007.

[38] Dr.K.Sri Rama Krishna, J.Lakshmi Narayana, Dr.L.Pratap Reddy, "ANN Models for Microstrip Line Synthesis and Analysis," *International Journal of Electrical Systems Science and Engineering*, pp. 196-200, 2008.

### Antenna Fabrication (Wet-Etching Techniques)

---

This appendix presents the fabrication or hardware implementation of the probe fed dual patch microstrip antenna described in the previous chapter. The antenna was fabricated and their return loss measured. As a validation of the results obtained from the simulation carried out, several designs proposed in previous section were fabricated.

#### 5.1 Hardware Implementation

Hardware Implementation involves three main steps.

1. Art work
2. Fabrication
3. Fabrication Process

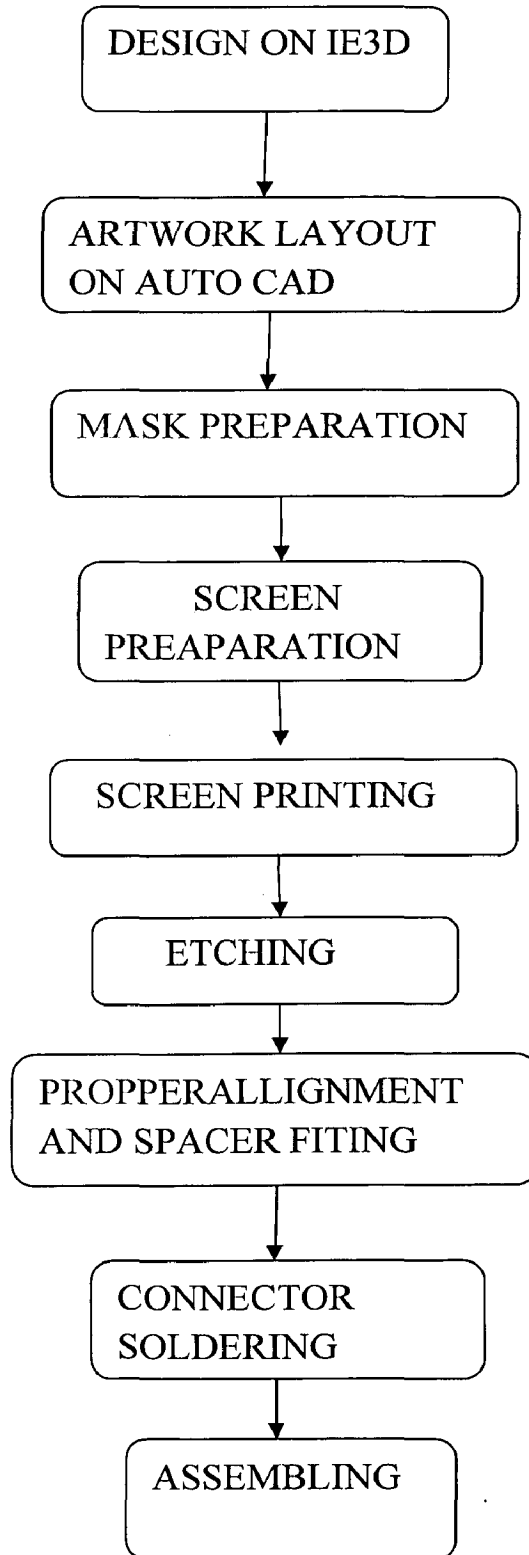
##### 5.1.1 Artwork

An artwork is the layout of all the copper printings to be done on the substrates. An artwork was prepared on Auto CAD with actual dimensions giving careful attention to tolerances to be taken in manufacturing. After an artwork was prepared, printout of these was taken with scale of 1:1 and the dimensions were checked with the help of vernier caliper having least count of 0.01 mm. Patch was printed on one side of the substrate and the opposite side of the substrate was etched completely. Coaxial fed was incorporated on aluminum plate of thickness 2mm of drilling holes. The tip of the coaxial fed was soldered at an appropriate point on the bottom patch antenna.

After an artwork, a mask was prepared. Then the images on the mask have to be transferred on the substrate. This was done by screen printing technique. The next step is to remove or etch out the unwanted portion of copper from the substrate. This was done by covering the layout image over the copper surface by dye and immersing the substrate in the ferric chloride solution. Uncovered portion of the copper dissolves into the solution and the copper layout remains on the substrate. Ferric chloride solution, which is stirred occasionally to increase the speed of the etching. After the etching is completed, the dye on the substrate is removed with the help of solvent to expose the patch and ground plane.

### 5.1.2 Fabrication

Steps involve in the fabrication are shown in the following flow chart.



### **5.1.3 Fabrication Process**

The flow of the fabrication process started with the mask generation on the transparency. AutoCAD software was used to draw the actual dimension of the antenna based on the configuration in the simulation. The transparency is then attached to the FR4 material and placed under the UV light for about 50 ~ 90 seconds. Here the mask unprotected area is exposed to the UV photo leaving the silicon dioxide layer on the top. Then silicon oxide etch process is carried out to remove the areas of silicon dioxide unprotected by the photo-resist to remove the SiO<sub>2</sub> and expose the silicon underneath. This is done by soaking the material in the developer solution for about 10 minutes.

### **5.2 Photolithography Procedure:**

Preparation of Mask using CAD tools:

After finalizing the circuit, note down the dimensions of the designed circuit. Draw the layout in IntelliCAD software loaded in your lab computer. While drawing the layout of the circuit in IntelliCAD, pay special attention to make unexposed portion of the circuit as closed structure. Save this layout as .dxf file and import it in another software tool available in lab which will convert your unexposed closed region into a polygon. This portion will be filled and circuit (which will be exposed by UV light in lithography) will be transparent. Take print out using 1:1 ratio on transparent. Further clarification will be given in laboratory.

**Step I:** Cleaning of Glassware and other utensils used in laboratory. Clean the copper laminate used in MIC using powdered soap and rinse it under running water. Use heat converter to dry the substrate and other glassware. Acetone can be used to further clean the substrate.

**Step II:** Take a small volume of Negative Photo resists (Negative PR) and place it on substrate. Use Spin Coating system to coat the PR on substrate and dry it in oven at 100 C for – 10 minutes.

**Step III:** Align the Photo Mask which contains layout of circuit on the coated side of substrate and use tape to fix it with substrate.

**Step IV:** Expose the circuit for 2 to 2.5 minute under UV light.

**Step V:** Remove the mask from substrate and develop the exposed circuit in developer (TCE) for 1-1.5 minutes and then dip it in fixer (Acetone) for around 1 minute.

Step VI: Use Blue dye so that layout is clearly visible. Heat the circuit in oven at 100 C for 10 minutes.

Step VII: Use brown tape to protect ground plane of microstrip and etch it using FeCl<sub>3</sub> solution. Clean the circuit under running water and use acetone for further cleaning.

### **5.3 Measurement**

After fabrication process was finished, measurement was carried out to evaluate the antenna performance and the result was compared with the simulation result. Return loss of the antenna was measured using ROHDE & SCHWARZ Vector Network Analyzer operating in 10 MHz to 40 GHz band at space application and satellite communications.

#### **5.3.1 Return Loss (S11) Measurement**

The resonant frequency of an antenna can be determined from an investigation of the input impedance characteristics of the antenna as a function of frequency. At the resonance there is only real part of the input impedance and the imaginary part of the antenna vanishes.

In order to sure that no radiation was received by the antenna during the impedance measurement the antenna was placed in front of network analyzer and care had been taken that there is no reflecting surface and no movement of anybody in the front of the antenna. The antenna had been connected the network analyzer. Before the antenna was connected, the set up was calibrated using open, short and broadband loads. This was done in order to make sure that it is the impedance of the antenna and not the impedance of the antenna and the coaxial cable that is measured. And print out were taken is shown below.

#### **5.3.2 Return Loss**

The return loss (RL) is a parameter which indicates the amount of power that is lost to the load and does not return as a reflection. As already known, waves are reflected leading to the formation of standing waves, when the transmitter and antenna impedance do not match. Hence the RL is a parameter similar to the VSWR to indicate how well the matching between the transmitter and the antenna has taken place. The RL is defined as

$$RL = -20 \log|\Gamma|$$



For perfect matching between the transmitter and the antenna,  $\Gamma = 0$  and  $RL = \infty$  which means no power is reflected back, while  $\Gamma = 1$  has an  $RL = 0$ , which implies that all the incident power is reflected. In practical application, a VSWR of 2 is acceptable, corresponds to an RL of -9.5 dB or 11% power reflection.

## MATLAB Program

---

### 1. Analysis modeling

```
1. P = [total input data];
2. T= [total target];
3. net = newff([7.5000 11.000;7.5000 11.000;1 13.1;1 3;6 9;6 9;1 4.2;1 3],[25 2],{'tansig'
    'purelin'});
4. % net.trainParam.mc=0.05;
5. % net.trainParam.goal=.0001;
6. % net.trainParam.show = 100;
7. net.trainParam.lr = 0.01;
8. net.trainParam.epochs =1000;
9. % net.trainParam.time =1000;
10. % plot{[1;115],p,'!',[1;115],p,'*'}
11. % save backward net t p
12. % load backward
13. [net,tr] = train(net,p,t);
14. y=sim(net,p);
15. train_error=mse(y-t)
16. f = sim(net,p)
17. p1=[8;8;3.2;1.5;6.9;6.9;1.2;2.1]
18. t1=[9.8667;14.4]
19. f1=sim(net,p1)
20. test_error=mse(f1-t1)
```

## 2. Design modeling

```
1. p=[total input data];
2. t=[total target];
3. net = newff([8.4 12.3333;12.2 17.8667;1 13.1;1 3;1 4.2;1 3],[25 2],{'tansig' 'purelin'});
4. % net.trainParam.goal=.0001;
5. % net.trainParam.show = 100;
6. net.trainParam.mc=0.6;
7. net.trainParam.lr = 0.1;
8. net.trainParam.epochs =1000;
9. % net.trainParam.time =1000;
10. % plot{[1;115],p,';', [1;115],p,'*'}
11. % save backward net t p
12. % load backward
13. [net,tr] = train(net,p,t);
14. y=sim(net,p);
15. train_error=mse(y-t)
16. d = sim(net,p)
17. p1=[11.5333;16.9333;2.2000;1.5300;1.0000;1.5300]
18. t1=[8;6.9]
19. d1=sim(net,p1)
20. test_error=mse(d1-t1)
```

Table

Various Input Parameters of the Dual Patch Microstrip Antenna

W1 (mm)	L1 (mm)	Ep1	H1 (mm)	W2 (mm)	L2 (mm)	Ep2	H2 (mm)	Ep3	H3 (mm)	Xp (mm)	Yp (mm)
7.5	7.5	1	1	6	6	1	1	2.2	3.09	2.5	2.5
8	8	1.2	1.1	6.1	6.1	1.07	1.1	2.2	3.09	2.5	2.5
8.1	8.1	1.22	1.2	6.2	6.2	1.2	1.2	2.2	3.09	2.5	2.5
8.2	8.2	1.82	1.3	6.3	6.3	1.22	1.3	2.2	3.09	2.5	2.5
8.3	8.3	1.88	1.35	6.4	6.4	1.82	1.4	2.2	3.09	2.5	2.5
8.4	8.4	1.93	1.4	6.5	6.5	1.88	1.5	2.2	3.09	2.5	2.5
8.5	8.5	2	1.5	6.6	6.6	1.93	1.53	2.2	3.09	2.5	2.5
8.6	8.6	2.1	1.53	6.7	6.7	2	1.6	2.2	3.09	2.5	2.5
8.7	8.7	2.17	1.6	6.8	6.8	2.1	1.7	2.2	3.09	2.5	2.5
8.8	8.8	2.2	1.7	6.9	6.9	2.16	1.8	2.2	3.09	2.5	2.5
8.9	8.9	2.25	1.8	7	7	2.17	1.9	2.2	3.09	2.5	2.5
9	9	2.26	1.9	7.1	7.1	2	2	2.2	3.09	2.5	2.5
9.1	9.1	2.32	2	7.2	7.2	2.2	2.2	2.2	3.09	2.5	2.5
9.2	9.2	2.35	2.2	7.3	7.3	2.25	3	2.2	3.09	2.5	2.5
9.3	9.3	2.39	3	7.4	7.4	2.35	1.53	2.2	3.09	2.5	2.5
9.4	9.4	2.42	2.2	7.5	7.5	3	1.53	2.2	3.09	2.5	2.5
9.5	9.5	2.44	2.5	7.6	7.6	4.2	1.53	2.2	3.09	2.5	2.5
9.8	9.8	2.54	1.53	7.7	7.7	1	1.53	2.2	3.09	2.5	2.5
10	10	2.55	1.53	7.8	7.8	1	1.53	2.2	3.09	2.5	2.5
11	11	2.6	1.53	7.9	7.9	1	1.53	2.2	3.09	2.5	2.5
8	8	2.65	1.53	8	8	1	1.53	2.2	3.09	2.5	2.5
8	8	3	1.53	8.5	8.5	1	1.53	2.2	3.09	2.5	2.5
8	8	3.2	1.53	9	9	1	1.53	2.2	3.09	2.5	2.5
8	8	3.8	1.53	6.9	6.9	1	1.53	2.2	3.09	2.5	2.5

8	8	4.2	1.53	6.9	6.9	1	1.53	2.2	3.09	2.5	2.5
8	8	5.75	1.53	6.9	6.9	1	1.53	2.2	3.09	2.5	2.5
8	8	7.5	1.53	6.9	6.9	1	1.53	2.2	3.09	2.5	2.5
8	8	10	1.53	6.9	6.9	1	1.53	2.2	3.09	2.5	2.5
8	8	11.9	1.53	6.9	6.9	1	1.53	2.2	3.09	2.5	2.5